



저작자표시-비영리-변경금지 2.0 대한민국

이용자는 아래의 조건을 따르는 경우에 한하여 자유롭게

- 이 저작물을 복제, 배포, 전송, 전시, 공연 및 방송할 수 있습니다.

다음과 같은 조건을 따라야 합니다:



저작자표시. 귀하는 원저작자를 표시하여야 합니다.



비영리. 귀하는 이 저작물을 영리 목적으로 이용할 수 없습니다.



변경금지. 귀하는 이 저작물을 개작, 변형 또는 가공할 수 없습니다.

- 귀하는, 이 저작물의 재이용이나 배포의 경우, 이 저작물에 적용된 이용허락조건을 명확하게 나타내어야 합니다.
- 저작권자로부터 별도의 허가를 받으면 이러한 조건들은 적용되지 않습니다.

저작권법에 따른 이용자의 권리는 위의 내용에 의하여 영향을 받지 않습니다.

이것은 [이용허락규약\(Legal Code\)](#)을 이해하기 쉽게 요약한 것입니다.

[Disclaimer](#)

**The radio-sensitizing effect and tumor  
growth inhibition by cystine/glutamate  
transporter (system  $x_c^-$ ) inhibition in  
glioblastoma**



Hong In Yoon

Department of Medical Science

The Graduate School, Yonsei University

**The radio-sensitizing effect and tumor  
growth inhibition by cystine/glutamate  
transporter (system  $x_c^-$ ) inhibition in  
glioblastoma**

Directed by Professor Chul Hoon Kim

The Doctoral Dissertation submitted to the  
Department of Medical Science,  
the Graduate School of Yonsei University  
in partial fulfillment of the requirements for the degree of  
Doctor of Philosophy

Hong In Yoon

December 2015

This certifies that the Doctoral Dissertation  
of Hong In Yoon is approved.

---

Thesis Supervisor: Chul Hoon Kim

---

Thesis Committee Member #1: Dong Goo Kim

---

Thesis Committee Member #2: Nam Hoon Cho

---

Thesis Committee Member #3: Bae Hwan Lee

---

Thesis Committee Member #4: Yong Bae Kim

The Graduate School  
Yonsei University

December 2015

## ACKNOWLEDGEMENTS

우선 제 인생의 갈 길을 인도해주시고 믿음을 주신 하나님께 감사와 영광을 드립니다.

Physician-scientist 과정에 참여할 수 있는 기회를 주시고, 지적 성장의 즐거움, 연구자로서의 자세와 소양을 기르고 사회 구성원으로서의 책임과 소임을 다 할 수 있도록 큰 가르침을 주신 김철훈 교수님께 진심으로 감사 드립니다. 또한 본 연구와 논문을 위하여 많은 조언과 격려를 베풀어주신 심사위원 교수님들께 깊은 감사 드립니다. 기초 연구에 대한 식견과 안목을 넓혀 주시고 과학자가 걸어가야 할 정도를 몸소 실천하시어 가르침을 주신 김동구 교수님 진심으로 감사 드립니다. 논문의 계획 단계부터 완성까지 많은 조언을 해주신 조남훈 교수님 진심으로 감사 드립니다. 생각지도 못 했던 부족한 부분을 항상 가르쳐 주셔서 이 학위 논문의 완성도를 더욱 높여 주신 이배환 교수님께 진심으로 감사 드립니다. 전공의 시절부터 박사 학위를 마무리하는 이 순간까지도 방사선종양학 의사로서 갖추어야 할 지식을 쌓고 인격을 계발할 수 있도록 가르쳐 주신 김용배 교수님께 감사 드립니다. 약리학교실원으로서 자부심을 갖도록 해주신 안영수 교수님, 이민구 교수님, 박경수 교수님, 김주영 교수님, 김형범 교수님과 지현영 교수님 감사합니다.

방사선종양학 전문의로서의 자긍심과 정체성을 일깨워 주신 김귀언 교수님, 서창욱 교수님, 성진실 교수님, 이창걸 교수님, 금기창 교수님, 조재호 교수님, 이익재 교수님, 금웅섭 교수님과 정암희 선생님들께 감사 드립니다. 전공의 1년차 때부터 지금까지

항상 친 형처럼 옆에서 지지해주고 든든한 큰 힘이 되어준 김준원 교수님께 진심으로 감사 드립니다. 마음이 정말 잘 통하는 가족 같은 후배 장지석 선생님 고맙습니다. 학위 기간 동안에 연구 진행에 큰 도움 주신 이은정 박사님 감사 드립니다. 그리고 미처 다 언급하지 못한 연세대학교 의과대학 방사선종양학교실 의국 후배님들 고맙습니다.

연세대학교 의과대학 약리학교실 신경과학 연구실에서 만나 5년동안 함께 생활하면서 회로애락을 함께 하며 큰 힘이 되어준 문여정 박사님과 임영신 박사님께 특히 감사드리며, 권오빈 박사님, 신소라 박사님, 조아련 박사님, 조호진, 이정호, 한웅수, 오소라, 서제호, 윤종진, 임지수 선생님에게도 감사 드립니다.

Physician-scientist 과정을 함께 하며 많은 어려움을 같이 이겨내며 즐겁고 행복한 추억을 쌓은 이찬주, 정진세, 박광환 박사님, 박형순, 정은석, 유정환, 전익현, 김한상 선생님 감사합니다. 특히, 어려운 상황에서도 종양학 스터디를 같이 하며 학구열을 불태운 박형순, 김한상, 차용훈 선생님 진심으로 감사합니다. 그외 다 언급하지 못한 physician-scientist 후배님들 고맙습니다.

박사 학위 취득을 진심으로 축하해준 친구들 감사합니다. 생각만으로도 기쁨을 주는 인생 최고의 친구 용국, 그리고 성남고 동기 정만, 영민, 성훈, 세준, 세호, 연세의대 규호, 홍상, 상현, 동진, 창명, 경제, 상훈, 공명, 병주, 호준, 훈, 모세, 희태, 해윤, 주원, 지선 등등 진심으로 감사합니다.

언제나 아낌없는 사랑과 헌신을 주신 사랑하는 부모님께 감사 드립니다. 제 부모님만큼 제게 아낌없는 사랑을 주시는

사랑하는 장모님께도 감사 드립니다. 항상 곁에서 사랑으로 절  
보살펴주며, 특히 대학원 생활 중에 언제나 흔들림 없이 정진할 수  
있도록 정신적으로 지지해준 사랑하는 아내 정운선에게 이 학위  
논문을 바칩니다. 그리고 태어난 그 날부터 항상 힘이 되어주는  
사랑하는 보물, 준우와 준영에게 고마운 마음을 담아 이 논문과  
함께 사랑을 전합니다. 힘든 타국 생활을 하면서도 관심과 격려를  
보내준 사랑하는 동생 홍일에게 조금만 더 힘내자는 말과 함께  
감사의 마음을 전합니다. 많은 관심과 격려를 해주신 처형들과  
동서 형님들 감사 드립니다. 끝으로 바쁘다는 이유로 많이 뵙지 못  
한 친가와 외가 친척들에게도 감사의 마음을 전합니다.



2015년 12월

윤 홍 인

# TABLE OF CONTENTS

<b>ABSTRACT</b> .....	1
<b>I. INTRODUCTION</b> .....	3
1. Glioblastoma treatment and prognosis .....	4
2. Ionizing radiation, DNA damage, and radio-sensitivity .....	5
3. System $x_c^-$ .....	7
A. System $x_c^-$ composition and function .....	7
B. System $x_c^-$ in cancer and resistance to cancer treatment .....	7
C. System $x_c^-$ affects cell growth in glioblastoma .....	9
D. System $x_c^-$ and cancer cell migration .....	10
4. The purpose of this study .....	11
<b>II. MATERIALS AND METHODS</b> .....	13
1. Glioblastoma cell lines and culture .....	13
2. Cortical astrocytes .....	13
3. Cell irradiation .....	14
4. Western blotting .....	14
5. Measurement of intracellular GSH level .....	15
6. RNA preparation and cDNA conversion .....	15
7. Real-time PCR .....	16
8. $\gamma$ -H2AX foci formation .....	17
9. Clonogenic (colony formation) assay .....	18
10. Wound healing ( <i>in vitro</i> scratch) assay .....	19
11. MTT cell viability assay .....	19
12. Immunohistochemistry .....	20
13. Statistical analysis .....	21

<b>III. RESULTS</b> .....	22
1. System $x_c^-$ inhibition and improved radio-sensitivity <i>in vitro</i> .....	22
A. System $x_c^-$ inhibition in glioblastoma <i>in vitro</i> .....	22
(A) Sulfasalazine inhibits xCT from system $x_c^-$ in glioblastoma <i>in vitro</i> .....	22
(B) xCT inhibition induces a decrease in intracellular GSH levels in glioblastoma <i>in vitro</i> .....	22
(C) Dose determination using the cell viability assay.....	24
B. Irradiation combined with system $x_c^-$ inhibition increased DSB compared to irradiation alone in glioblastoma <i>in vitro</i> ....	24
C. System $x_c^-$ inhibition enhanced radio-sensitivity in glioblastoma <i>in vitro</i> .....	25
D. Summary .....	30
2. System $x_c^-$ inhibition and cell migration through the change of mesenchymal markers .....	31
A. System $x_c^-$ inhibition reduced the cell migration in glioblastoma <i>in vitro</i> .....	31
B. System $x_c^-$ inhibition decreased the expression levels of mesenchymal markers in glioblastoma <i>in vitro</i> .....	33
(A) IR increased the expression of the TCGA-based mesenchymal markers, CD44 and YKL-40 <i>in vitro</i> .....	33
(B) System $x_c^-$ inhibition decreased the mRNA expression of mesenchymal markers in glioblastoma <i>in vitro</i> .....	34
(C) System $x_c^-$ protein expression was higher in mesenchymal glioblastoma than in proneural glioblastoma .....	43
C. Summary .....	43

**IV. DISCUSSION** ..... 47

**V. CONCLUSION** ..... 53

**REFERENCES** ..... 54

**ABSTRACT (IN KOREAN)** ..... 61

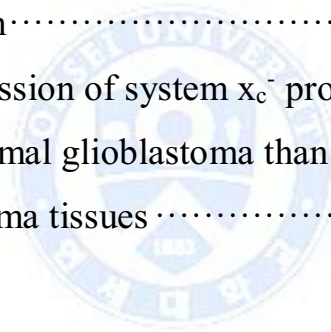
**PUBLICATION LIST** ..... 64



## LIST OF FIGURES

<b>Figure 1.</b> Irradiation induces ROS production, which results in DNA DSB .....	6
<b>Figure 2.</b> System $x_c^-$ is a cystine/glutamate transporter .....	9
<b>Figure 3.</b> System $x_c^-$ inhibition by sulfasalazine (SAS) in glioblastoma and astrocytes .....	23
<b>Figure 4.</b> Decrease in intracellular GSH induced by xCT inhibition in glioblastoma .....	26
<b>Figure 5.</b> Determination of the sulfasalazine (SAS) dose in A172 and U87-MG cells .....	27
<b>Figure 6.</b> The combination of irradiation with sulfasalazine (SAS) treatment increased DSB in glioblastoma .....	28
<b>Figure 7.</b> System $x_c^-$ inhibition enhanced radio-sensitivity in glioblastoma .....	29
<b>Figure 8.</b> System $x_c^-$ inhibition reduced the cell migration in glioblastoma .....	32
<b>Figure 9.</b> Sulfasalazine cytotoxicity did not affect the cell migration .....	34
<b>Figure 10.</b> Irradiation increased the expression of TCGA-based mesenchymal markers, CD44 and YKL-40 .....	35
<b>Figure 11.</b> System $x_c^-$ inhibition decreased the <i>SNAIL</i> mRNA expression in glioblastoma .....	36

<b>Figure 12.</b> System $x_c^-$ inhibition decreased vimentin mRNA expression in glioblastoma .....	37
<b>Figure 13.</b> System $x_c^-$ inhibition decreased N-cadherin mRNA expression in glioblastoma .....	39
<b>Figure 14.</b> System $x_c^-$ inhibition decreased alpha-SMA mRNA expression in glioblastoma .....	41
<b>Figure 15.</b> System $x_c^-$ inhibition decreased FAP mRNA expression in glioblastoma .....	42
<b>Figure 16.</b> Sulfasalazine cytotoxicity did not affect mRNA expression .....	44
<b>Figure 17.</b> The expression of system $x_c^-$ protein was higher in mesenchymal glioblastoma than in proneural glioblastoma tissues .....	45



## ABSTRACT

### **The radio-sensitizing effect and tumor growth inhibition by cystine/glutamate transporter (system $x_c^-$ ) inhibition in glioblastoma**

Hong In Yoon

*Department of Medical Science  
The Graduate School, Yonsei University*

(Directed by Professor Chul Hoon Kim)

Glioblastoma is the most aggressive brain tumor. Despite existing multimodal therapy, new therapeutic strategies are required. System  $x_c^-$ , composed of a light-chain subunit (xCT, SLC7A11) and a heavy chain subunit (CD98hc, SLC3A2), releases glutamate outside the cell and concurrently uptakes cystine in the cell at a 1 to 1 ratio. The increased intracellular cystine, due to uptake by system  $x_c^-$ , is transformed into glutathione (GSH) that is one of the most important antioxidants in cancer cells, contributing to cancer cell survival and proliferation. So, I investigated that the inhibition of system  $x_c^-$  could improve the radio-sensitivity and reduce the cell growth and migration in glioblastoma.

Herein, I show that system  $x_c^-$  inhibition could enhance radio-sensitivity and repress glioblastoma progression and invasion. System  $x_c^-$  inhibition induces a decrease in intracellular GSH in glioblastoma.

Irradiation combined with system  $x_c^-$  inhibition increases DNA double strand breaks (DSB) than that with irradiation alone in glioblastoma. The combination of irradiation and system  $x_c^-$  inhibition resulted in a significantly lower surviving fraction at each dose than irradiation alone.

Irradiation could induce the change of mesenchymal markers. Additionally, the expression of the Cancer Genome Atlas (TCGA)-based markers of mesenchymal glioblastoma, CD44 and YKL-40, was elevated after the irradiation. System  $x_c^-$  inhibition reduced cell migration through the change of mesenchymal markers in glioblastoma. Although irradiation significantly increased cell movement, system  $x_c^-$  inhibition blocked the radiation-induced cell migration. System  $x_c^-$  inhibition is significantly related to decrease in mesenchymal markers, including *SNAIL*, vimentin, N-cadherin, alpha-SMA and FAP in glioblastoma. System  $x_c^-$  protein expression was significantly higher in the mesenchymal than that in the proneural human glioblastoma specimens.

In conclusion, these findings demonstrate that system  $x_c^-$  inhibition in combination with irradiation could decrease cystine uptake and GSH, inducing an increase in DNA DSB. System  $x_c^-$  inhibition could enhance radio-sensitivity in glioblastoma. In addition, system  $x_c^-$  inhibition prevented the radiation-induced cell migration and affected mesenchymal features, which are adverse prognostic factors in glioblastoma. Taken together, my results indicate that the combination of radiation therapy (RT) and system  $x_c^-$  inhibition could improve therapeutic outcomes in glioblastoma.

---

**Key words: System  $x_c^-$ , Cystine/glutamate transporter, Irradiation, Radio-sensitivity, Migration**

# **The radio-sensitizing effect and tumor growth inhibition by cystine/glutamate transporter (system $x_c^-$ ) inhibition in glioblastoma**

Hong In Yoon

*Department of Medical Science  
The Graduate School, Yonsei University*

(Directed by Professor Chul Hoon Kim)



## **I. INTRODUCTION**

Despite multimodal approaches for the treatment of glioblastoma, including radical resection followed by postoperative radiotherapy (RT) and temozolomide, new therapeutic strategies to enhance radio-sensitivity are needed and investigated due to poor prognosis and radio-resistance of glioblastoma.

Ionizing radiation (IR) causes deoxyribonucleic acid (DNA) double strand breaks (DSB). The major mechanism of IR-induced DNA damage involves the indirect induction of reactive oxygen species (ROS), which is responsible for 70% of total IR-induced DNA DSB. This implies that enhancing indirect actions of IR could improve radio-sensitivity.

System  $x_c^-$ , a cystine/glutamate antiporter, releases glutamate outside the cell and concurrently uptakes cystine in the cell at a 1 to 1 ratio.<sup>1-5</sup> Intracellular

cystine is then transformed into cysteine and finally glutathione (GSH), one of the most important antioxidants in mammalian cells as well as cancer cells, which protects cancer cells from intracellular ROS generated by external insults such as IR.<sup>6,7</sup> In glioblastoma, the expression levels of system  $x_c^-$  are higher than those in normal astrocytes. A retrospective study using surgical specimens from patients with glioblastoma demonstrated that the increase in system  $x_c^-$  expression level was significantly associated with poor prognosis.<sup>8</sup> It was reported that when the function of system  $x_c^-$  is inhibited, intracellular GSH levels decreased, resulting in a decrease in tumor growth.<sup>9</sup> Thus, studies investigating whether combining RT with a system  $x_c^-$  inhibitor could enhance the radio-sensitivity of glioblastoma and improve therapeutic effects are necessary. In addition, some studies demonstrated that malignant glioma can release glutamate by system  $x_c^-$ , inducing excitotoxicity in normal neurons and astrocytes and facilitating tumor progression.<sup>10,11</sup>

I hypothesized that system  $x_c^-$  inhibition could increase ROS effects and DNA damage after IR in glioblastoma by enhancing radio-sensitivity. In addition, I hypothesized that the inhibition of system  $x_c^-$  could repress glioblastoma progression and invasion. So, I evaluated that system  $x_c^-$  would enhance the radio-sensitivity and reduce the cell growth and migration in glioblastoma.

## 1. Glioblastoma treatment and prognosis

Glioblastoma is the most common malignant brain tumor.<sup>12,13</sup> This disease is the most aggressive brain tumor associated with poor survival despite combination therapy of radical resection followed by RT and temozolomide.<sup>14,15</sup>

The standard treatment for newly diagnosed patients with glioblastoma is radical resection followed by postoperative RT combined with chemotherapy.<sup>16</sup> RT is typically delivered as 60 Gy per 30 fractions to the patients' postoperative tumor bed or residual tumors. Temozolomide, an oral DNA alkylating agent, is administered concurrently with radiotherapy and in an adjuvant setting after RT. In spite of aggressive treatment, glioblastoma of infiltrative features and radio-resistance commonly result in disease progression.<sup>17-19</sup> Thus, new therapeutic strategies to enhance radio-sensitivity are required.

## 2. Ionizing radiation, DNA damage, and radio-sensitivity

IR carries enough energy to free electrons to ionize atoms or molecules. IR includes a photon radiation such as  $\gamma$ -ray, X-ray, and the higher energy of ultraviolet part of the electromagnetic spectrum.

DNA damage is an alteration in the chemical structure of DNA, including a break in one or both strands of DNA and a missing base from the DNA backbone. DNA damage can be induced by ROS, reactive nitrogen species, reactive carbonyl species, lipid peroxidation products, chemotherapy such as alkylating agents, and IR.<sup>20</sup>

IR causes DSB, the most deleterious type of DNA damage, which leads to cell death if DNA repair does not occur.<sup>21</sup> The mechanism of DNA damage by IR consists of direct and indirect actions (Figure 1). Direct action occurs when particle radiation such as  $\alpha$ , or  $\beta$  particles, neutron, proton or carbon ion break the sugar phosphate backbones or the base pairs of the DNA. In the indirect action, when IR such as photon radiation is absorbed in a biological material, ROS are produced. These ROS are highly reactive molecules. ROS could break

chemical bonds in DNA, produce chemical changes, and initiate the chain of events that results in biological damage. This represents the indirect effect of photon radiation on DNA, which constitutes 70% of total DNA DSB. This finding demonstrates that enhancing the indirect action of radiation could improve radio-sensitivity.

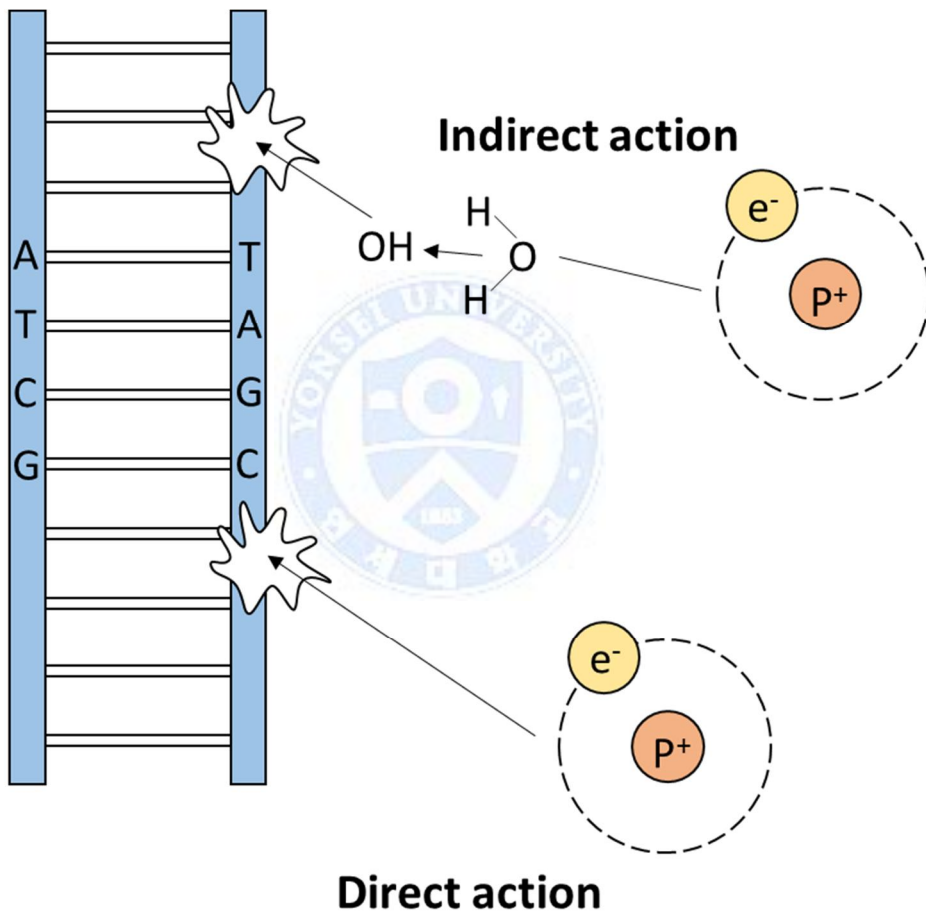


**Figure 1. Irradiation induces ROS production, which results in DNA DSB.**  
The mechanism of DNA damage by IR consists of direct and indirect actions by x-ray.

### 3. System $x_c^-$

#### A. System $x_c^-$ composition and function

System  $x_c^-$ , a cystine/glutamate antiporter, releases glutamate outside the cell and concurrently uptakes cystine in the cell at a 1 to 1 ratio (Figure 2).<sup>1-5</sup> System  $x_c^-$  is one of the representative solute carriers and one of the representative amino acid transporters overexpressed in tumor cells.<sup>22</sup> System  $x_c^-$  is composed of a light-chain subunit (xCT, SLC7A11) and a heavy chain subunit (CD98hc, SLC3A2). xCT expression levels are known to correlate with system  $x_c^-$  activity, because xCT determines the substrate specificity and efficiency of system  $x_c^-$ . The increase of intracellular cystine by system  $x_c^-$  results in the production of cysteine and, finally, GSH, which is one of the most important antioxidants in mammalian cells.<sup>23</sup>

#### B. System $x_c^-$ in cancer and resistance to cancer treatment

Generally, cancer cells generate a substantial amount of ROS due to their enhanced metabolism and growth. Intracellular antioxidants play a critical role in preventing ROS damage. GSH is known to be representative of intracellular antioxidants and elevated in cancer cells. In addition, the elevated GSH in cancer cells could protect cancer cells from intracellular ROS generated by external insults such as IR.<sup>6,7,24</sup> Thus, system  $x_c^-$  expression level increases in various types of cancer, because surface expression of system  $x_c^-$  is critical for the uptake of cystine required for intracellular GSH synthesis and the

maintenance of the redox balance.<sup>25</sup> Therefore, modulation of the xCT activity of system x<sub>c</sub><sup>-</sup> has been considered as a new cancer therapeutic target.<sup>22</sup>

Several studies demonstrate that system x<sub>c</sub><sup>-</sup> contributes to cancer growth, invasion, progression, and metastasis in various types of cancer.<sup>25-28</sup> In a study using an esophageal squamous cell cancer cell line, depletion of xCT using a drug inhibitor could inhibit cancer cell metastasis via the caveolin-1/ $\beta$ -catenin pathway.<sup>26</sup> Some studies reported that the interaction between system x<sub>c</sub><sup>-</sup> and CD44, which is an adhesion molecule expressed in cancer stem-like cells, is important for tumor growth, progression, and resistance to cancer therapy.<sup>25,27,28</sup> Ishimoto *et al.* demonstrated that a CD44 variant interacts with xCT and controls reduced GSH intracellular levels.<sup>25</sup> A high level of CD44 expression is associated with an enhanced capacity for GSH synthesis and defense against ROS in gastro-intestinal cancer.<sup>25</sup> Yoshikawa *et al.* showed that xCT inhibition selectively induces the apoptosis of CD44v-expressing tumor cells that are resistant to EGFR-targeted therapy in head and neck squamous cell carcinoma.<sup>28</sup> Combination with xCT and EGFR inhibitors resulted in a synergistic reduction of EGFR-expressing tumor growth. Furthermore, system x<sub>c</sub><sup>-</sup> induced radio-resistance and chemo-resistance have been reported in several studies for various types of cancer.<sup>26,29-31</sup>

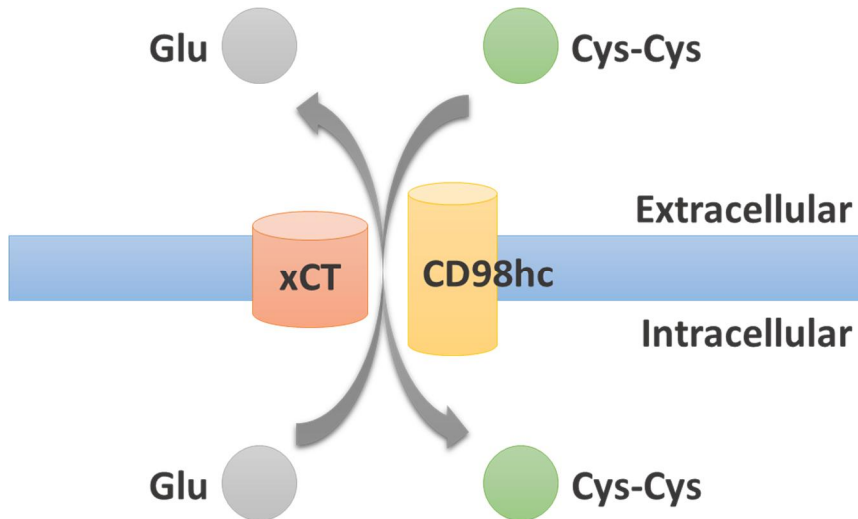


**Figure 2. System  $x_c^-$  is a cystine/glutamate transporter.** System  $x_c^-$  is composed of a light-chain subunit (xCT, SLC7A11) and a heavy chain subunit (CD98hc, SLC3A2). Through system  $x_c^-$ , cystine is transported into cells in exchange for the release of glutamate at a one to one ratio.

### C. System $x_c^-$ affects cell growth in glioblastoma

GSH is abundantly present in human brain tumors.<sup>32</sup> Cystine necessary to produce GSH is also provided through system  $x_c^-$  in glioma. According to previous studies, the expression levels of system  $x_c^-$  in glioblastoma are higher than those in normal astrocytes.<sup>9</sup> It was reported that when system  $x_c^-$  function is inhibited, intracellular GSH levels as well as tumor growth decreased.<sup>9</sup>

A retrospective study using surgical specimens from patients demonstrated that the increase in system  $x_c^-$  expression levels was significantly associated with poor prognosis.<sup>8</sup> In normal brain areas, weak xCT expression was observed in leptomeningeal cells and scattered astrocytes. Among

glioblastoma specimens from 40 patients, 50% of patients showed strong expression of xCT. On multivariate analysis, strong expression of xCT was an independent prognostic factor for progression-free survival and overall survival. Recently, a study reported the mechanism of ROS-mediated therapeutic resistance in glioblastoma.<sup>33</sup> Microarray, Taqman, and functional assays used in this study demonstrated that therapeutic resistance was mediated by enhanced expression of the antioxidant response system x<sub>c</sub><sup>-</sup> catalytic subunit xCT.

Thus, in glioblastoma, studies are required to determine whether the combination of RT with a system x<sub>c</sub><sup>-</sup> inhibitor could enhance the radio-sensitivity and improve therapeutic effects. Inhibition of system x<sub>c</sub><sup>-</sup> would also allow the use of lower doses of RT by enhancing radio-sensitivity, thereby reducing RT-related toxicity and sequelae in the normal brain after RT for glioblastoma.

#### D. System x<sub>c</sub><sup>-</sup> and cancer cell migration

The effect of system x<sub>c</sub><sup>-</sup> in glioblastoma arises from cystine uptake as well as glutamate release. The extracellular glutamate released by system x<sub>c</sub><sup>-</sup> promotes glioma cell growth and destructs the adjacent normal tissue by inducing neuro-cytotoxicity and tumor expansion, facilitated by the activation of NMDA receptors.<sup>10,11,34-36</sup> Thus, system x<sub>c</sub><sup>-</sup> inhibition does not only affect the redox status, but also inhibits tumor growth through the decrease of glutamate release, which plays a critical role in reducing the progression and invasion of glioblastoma.

Several subtypes of glioblastoma, varying in molecular circuitry and biological behavior, have been identified. These include the proneural, neural, classical, and mesenchymal types.<sup>37,38</sup> Interestingly, each subtype harbors distinct

genetic aberrations and proteomic profiles. Glioblastoma subtypes appear to differ in their clinical courses and therapeutic responses. Among them, the proneural type harbors frequent mutations in p53, platelet-derived growth factor receptor A, and isocitrate dehydrogenase (IDH) 1. In contrast, the mesenchymal type is characterized by frequent mutations in the neurofibromatosis type 1 gene (NF-1). The signature of mesenchymal glioblastoma is known as YKL-40 and CD44 positive. Patients presenting proneural glioblastoma survive longer than patients with mesenchymal glioblastoma.<sup>39</sup>

In 2007, a study reported that IR induces changes associated with epithelial-mesenchymal transition (EMT) and increases cell motility of lung cancer cells.<sup>40</sup> Radiation induced an increase in  $\gamma$ -H2AX expression and a decrease in E-cadherin expression. After 48 hours following radiation, cell migration increased in the radiation group when compared to the control group.<sup>41</sup> In 2014, other study described that IR induces glial-mesenchymal transition similar to EMT and affects mesenchymal markers in malignant glioma (MG).<sup>42</sup> In 22 cases presenting clinically recurrent MG, the expression of the mesenchymal marker vimentin increased. Among the regulators of mesenchymal transition, snail elevation was observed in MG cells at 2 days after irradiation. CD44, a mesenchymal marker of glioblastoma, is known to enhance the stabilization and function of xCT and to promote tumor growth.<sup>25</sup>

#### 4. The purpose of this study

It is hypothesized that system x<sub>c</sub><sup>-</sup> inhibition could increase ROS effects and DNA damage after IR in glioblastoma and xCT inhibition could prevent glioblastoma migration. The aim of my study is to investigate the enhanced

radio-sensitivity and reduced cell growth and migration by system  $x_c^-$  inhibition in glioblastoma using glioblastoma cell-lines and human tissues.



## II. MATERIALS AND METHODS

### 1. Glioblastoma cell lines and culture

Glioma cells, U87-MG (human glioblastoma cell line, ATCC Number: HTB-14™, American Type Culture Collection, Manassas, VA, USA), and A172 cells (human glioblastoma cell line, ATCC Number: CRL-1620™, American Type Culture Collection) were used in this study. U87-MG cells were cultured in Eagle's Minimum Essential Medium (EMEM) supplemented with 10% fetal bovine serum (FBS) and 1% penicillin-streptomycin. A172 cells were cultured in Dulbecco's Modified Eagle's Medium (DMEM) supplemented with 10% FBS and 1% penicillin-streptomycin.

### 2. Cortical astrocytes

Cortical astrocytes were prepared from Sprague Dawley rats using a protocol described previously.<sup>43</sup> All protocols were approved by the Institutional Animal Care and Use Committee of Yonsei University Health System. The cortices, which were removed from early postnatal mice (postnatal days 1–3), were used, while the hippocampal formation, basal ganglia, and most of the meninges were discarded. Thereafter, the tissue was minced and incubated in 0.08% acetylated trypsin for 45–75 minutes at 37°C. The tissue was then dissociated by trituration and plated as a single-cell suspension on Primaria (Falcon) 35 mm dishes (10<sup>6</sup> cells/dish) in the plating medium (EMEM, Earle's salts) with supplements of 10% heat-inactivated horse serum, 10% FBS, glutamine (2 mM, added freshly), glucose (21 mM), and bicarbonate (38 mM).

After 5–7 days *in vitro*, non-glial cell division was stopped by 1–3 day of exposure to  $10^{-5}$  M cytosine arabinoside. The cells were moved into a maintenance medium similar to the plating medium, but lacking FBS. Subsequently, the medium was replaced on a biweekly schedule. The culture medium did not contain glutamate, except for that present in the serum. Based on the supplier's measurement of serum glutamate levels, the initial glutamate concentration in the maintenance medium was less than 20  $\mu$ M.

### 3. Cell irradiation

X-rad 320 (Precision X-Ray, North Branford, CT, USA) was used, operating at 320 kVp and 12.5 mA with 2.0 mm Al filtration and a dose rate of 4.76 cGy/sec.

### 4. Western blotting

The cells were washed twice with cold phosphate buffered saline (PBS) and lysed at 4°C for 15 minutes in PBS containing 1% Triton X-100 and the complete protease inhibitor mixture (Roche). The cell lysates were then cleared by centrifugation at  $12,000 \times g$  for 10 minutes at 4°C and protein concentrations were determined. The protein samples were resolved by SDS-polyacrylamide gel electrophoresis and transferred onto polyvinylidene fluoride membranes. The membranes were blocked with 0.5% non-fat milk plus 0.1% Tween 20 for 1 hour. After blocking, the membranes were incubated overnight at 4°C in primary antibodies, including an anti-human xCT (rabbit polyclonal antibody, ab37185, Abcam, Tokyo, Japan) (1:1000). Membranes were rinsed at least three times

with tris-buffered saline (TBS) and tween 20 (TBST) from 5 minutes each and were then incubated in 1% non-fat milk containing a horseradish peroxidase (HRP) conjugated secondary antibody for 2 hours at room temperature. After the final TBST wash, the membranes were suspended in an enhanced chemiluminescence solution (Pierce, Rockford, IL, USA) and exposed on film. Western blots were then scanned.<sup>44</sup>

## 5. Measurement of intracellular GSH level

Intracellular GSH levels were measured using the GSH assay kit (GSH-Glo™ Glutathione Assay, Promega, Madison, WI, USA) according to the manufacturer's instructions. Briefly, the medium from the wells of a 96-well plate was removed after plating cells and performing the required treatments. Then, 100 μL of prepared 1X GSH-Glo™ Reagent was added to each well. After, 30 minutes of incubation at room temperature, 100 μL of reconstituted Luciferin Detection Reagent was added to each well. After mixing briefly on a plate shaker, the plate was incubated for 15 minutes. Thereafter, the luciferase activity was measured by using a luminometer.

## 6. RNA preparation and cDNA conversion

For RNA preparation (RNeasy mini kit, Qiagen, Hilden, Germany), cells were disrupted in 600 μL of RLT buffer. The lysate was then centrifuged for 3 minutes in order to eliminate everything, but the supernatant. After adding 1 volume of 70% ethanol to the cleared supernatant, the sample was transferred to the RNeasy spin column and centrifuged at  $8,000 \times g$  for 15 sec. The RNeasy

spin column was centrifuged two more times at  $8000 \times g$  for 15 sec – once after adding 700  $\mu\text{L}$  of RW1 buffer and again after adding 500  $\mu\text{L}$  of RPE buffer. Then, 20  $\mu\text{L}$  of RNase-free water was added directly to the spin column membrane for RNA elution. Five hundred nanograms of RNA were used as the template for a 20  $\mu\text{L}$  cDNA synthesis using Superscript III (Invitrogen, Carlsbad, CA, USA).

## 7. Real-time PCR

Quantitative real-time PCR was carried out to measure the mRNA levels of xCT and mesenchymal markers. The expression of GAPDH mRNA served as an internal control. The real-time PCR reactions were performed with a 7300 Real-time PCR system (Applied Biosystems, Foster City, CA, USA) using fluorescent SYBR Green technology (Applied Biosystems) according to the manufacturer's instructions. Unique primer pairs from coding sequences were specifically identified using Primer Express (Applied Biosystems). The forward and reverse primers used to amplify the xCT, mesenchymal markers, and GAPDH were as follows: xCT, 5'- CCT CTT CAT GGT TGC CCT TTC-3' and 5'-ATG ACG AAG CCA ATC CCT GTA-3'; E-cadherin, 5'-TGA GTG TCC CCC GGT ATC TTC-3' and 5'-CAG TAT CAG CCG CTT TCA GAT TTT-3'; occludin, 5'-ATG GTT CAC AAA TAT ATG CCC TCT-3' and 5'-TCA TCA TAA ATG TGT TCC TTG TCC-3'; claudin-3, 5'-AAC ACC ATT ATC CGG GAC TTC TAC-3' and 5'-GTC TGT CCC TTA GAC GTA GTC CTT-3'; snail, 5'-ATC GGA AGC CTA ACT ACA GC-3' and 5'-CAG AGT CCC AGA TGA GCA TT-3'; vimentin, 5'-CGT ACG TCA GCA ATA TGA AAG TGT-3' and 5'-

GTG TCT TGG TAG TTA GCA GCT TCA-3'; fibronectin, 5'-AAG AGA CAG CTG TAA CCC AGA CTT-3' and 5'-AAG TGC AAT CAG TGT AAT TGT GGT-3'; alpha-smooth muscle actin (alpha-SMA), 5'-GAC AAT GGC TCT GGG CTC TGT AA-3' and 5'-ATG CCA TGT TCT ATC GGG TAC TT-3'; Fibroblast activation protein (FAP), 5'- GTA TTT GGA GTT GCC ACC TCT G-3' and 5'- GAA GGG CGT AAG ACA ATG CAC-3'; *GAPDH*, 5'-CCT CGA GAA ACC TGC CAA GTA T-3' and 5'-CTC GGC CGC CTG CTT-3'. Real-time PCR was carried out on 2  $\mu$ L of cDNA synthesized from 200 ng of total RNA. The ubiquitously expressed GAPDH was used as an endogenous control. The ratio of mesenchymal markers expression to GAPDH gene expression represents the relative expression level of mesenchymal markers. The  $2^{-\Delta\Delta CT}$  method was used to quantify the relative change.

#### 8. $\gamma$ -H2AX focus formation

For the  $\gamma$ -H2AX focus formation assay, 45 cells were plated on coverslips. Before irradiation, the cells were mock-treated with Dimethyl sulfoxide (DMSO) or treated with 0.25 mM sulfasalazine for 24 hours. The cells were irradiated with 2 or 10 Gy using X-RAD 320 (Precision X-Ray). After irradiation, the cells were fixed in 4% paraformaldehyde and incubated overnight with an anti- $\gamma$ -H2AX antibody (Millipore, Darmstadt, Germany). Cells were incubated in the dark with an FITC-labeled secondary antibody for 1 hour and then incubated in the dark with 4,6-diamidino-2-phenylindole (DAPI) for 10 minutes. Coverslips were then mounted with an antifade solution. Detection of fluorescence and acquisition of images were performed with a Zeiss LSM 700 confocal

fluorescence microscope. For each treatment condition,  $\gamma$ -H2AX foci were determined in at least 100 cells.

## 9. Clonogenic (colony formation) assay

Clonogenic assay for radiation survival experiments was performed as previously described.<sup>45,46</sup> Cells were plated in triplicate per data point into 6-well plates and then allowed to attach. Before irradiation, the cells were mock-treated with DMSO or treated with 0.25 mM sulfasalazine for 24 hours. The cells were irradiated with graded doses of X-rays, 0, 2, 4, and 6 Gy, using X-RAD 320. Immediately after irradiation, the cells were incubated in drug-free medium for 10–14 days to allow for the formation of colonies. Thereafter, the cells were stained with 0.5% crystal violet. The colonies were counted with a cutoff value of 50 viable cells, providing the percentage of survival as a function of the irradiation dose. The cell survival curve is defined as a relationship between the doses of the agent used to produce an insult and the fraction of cells retaining their ability to reproduce and calculated using a percentage of survival as a function of the dose. Thus, I calculated the plating efficacy (PE) and surviving fraction (SF). The PE is the ratio of the number of colonies to the number of cells seeded from the non-irradiated control plate. The SF is defined as the number of colonies that arise after treatment of the cells divided by the number of cells seeded multiplied by PE.

## 10. Wound healing (*in vitro* scratch) assay

Monolayer wound-healing (*in vitro* scratch) assay was performed by plating cells in 6-well plates according to previous studies.<sup>47</sup> Cells were seeded to confluence or near confluence (>90%) into 6-well plates. The confluent monolayers were scratched using a pipette tip. This allows imaging of both wound edges using the 10× objective of a light microscope. Thereafter, cells, which migrated after 24 hours, were imaged under the 10× objective and analyzed.

## 11. MTT cell viability assay

To evaluate the effect of system  $x_c^-$  inhibition on cell viability, cell viability was measured using 3-(4,5-Dimethyl-2-thiazolyl)-2,5-diphenyl-2H-tetrazolium bromide (MTT) according to the manufacturer's protocol (Dojindo Molecular Technologies, INC., Munich, Germany). A total of 5000 cells were plated in each well of 96-well plate with 100  $\mu$ L of growth medium. After incubation for 24 hours in a CO<sub>2</sub> incubator following sulfasalazine treatment and irradiation with 10 Gy, 10  $\mu$ L of MTT solution were added to each well. The plate was incubated at 37°C for 3 hours. Thereafter, 100  $\mu$ L of DMSO was added to dissolve the resulting MTT formazan. The absorbance was measured at 520–600 nm with a microplate reader.

## 12. Immunohistochemistry

Immunohistochemistry was performed using 3,3'-Diaminobenzidine (DAB) peroxidase substrate kit (SK-4100, Vector Laboratories, Inc., CA, USA). I obtained the human paraffin embedded tissue sections presenting proneural and mesenchymal glioblastoma from Professor S.H. Kim at the department of pathology in Yonsei University College of Medicine. For deparaffinization, slides were incubated in xylene for 24 hours at room temperature. Thereafter, the slides were incubated in fresh xylene for 15 minutes. This step was repeated. The slides were then incubated in 100%, 95%, 90%, 80%, and 70% ethanol for 15 minutes and then in distilled water for 5 minutes. The slides were incubated at 100°C for 20 minutes in 0.01 M sodium citrate buffer for antigen retrieval and then multiple washes were performed in PBS with gentle shaking. The slides were incubated in oxidation blocking buffer (200 mL methanol and 3 mL of 30% hydrogen peroxide) at room temperature. Thereafter, slides were washed three times in PBS for 5 minutes each. Each section was blocked with 400  $\mu$ L blocking solution for 1 hour at room temperature in a humidified chamber. The blocking solution was removed and 400  $\mu$ L of primary antibody against xCT (1:400, rabbit, polyclonal, abcam, Cambridge, UK) diluted in blocking solution was added to each section. The slides were incubated overnight at 4°C in a humidified chamber. After removal of the primary antibody solution, the slides were washed in PBS three times for 5 minutes each. Then, 400  $\mu$ L of biotinylated secondary antibody (rabbit) in blocking solution was added and incubated for 1 hour at room temperature in a humidified chamber. After 3 washes with PBS, signal amplification was performed using the avidin-biotin complex (ABC) according to manufacturer's instructions (PK-6101, Vector

Laboratories, Inc.). The ABC complex solution (500  $\mu$ L) was added to each section and incubated 1 for hour at room temperature in a humidified chamber. After 3 washes in PBS, 400  $\mu$ L of DAB solution was added to each section and monitored closely. After 1–2 minutes, acceptable staining intensity was obtained. The slides were immediately washed in PBS three times for 10 minutes each. Dehydration was then performed by incubation in 50%, 75%, 95%, 100% ethanol for 5 minutes and xylene for 20 minutes. At last, the samples were mounted with the Fisher Permount™ mounting medium and cover glasses (SP15-100, Fisher scientific, Pittsburgh, PA, USA).

### 13. Statistical analysis

All data are presented as mean  $\pm$  standard error of the mean (SEM). Data were analyzed with regard to statistical significance using an independent-samples t test and one-way analysis of variance followed by Bonferroni post-hoc test. A p-value  $<0.05$  was considered to be statistically significant.

### III. RESULT

#### 1. System $x_c^-$ inhibition and improved radio-sensitivity *in vitro*

##### A. System $x_c^-$ inhibition in glioblastoma *in vitro*

###### (A) Sulfasalazine inhibits xCT from system $x_c^-$ in glioblastoma *in vitro*

I used sulfasalazine as a potent selective competitive inhibitor of system  $x_c^-$ . After system  $x_c^-$  inhibition with sulfasalazine, the expression of xCT, the light chain of system  $x_c^-$ , was suppressed in A172 and U87-MG (Figure 3A). I also observed that xCT mRNA expression was significantly elevated by the decrease in xCT protein expression compared to controls (Figure 3B,  $p < 0.001$  in both cell lines).

###### (B) xCT inhibition induces a decrease in intracellular GSH levels in glioblastoma *in vitro*

To investigate whether system  $x_c^-$  inhibition induces a decrease in intracellular GSH levels, I measured intracellular GSH levels in glioblastoma and astrocytes. System  $x_c^-$  inhibition by sulfasalazine caused a dose-dependent reduction of GSH levels in A172 and U87-MG cells. At 24 hours following SAS treatment, the intracellular GSH levels decreased as the dose increases in both cells (Figure 4A,  $p < 0.001$ ). After 0.25 mM sulfasalazine treatment, the intracellular GSH levels decreased as time goes on in both cells (Figure 4B,  $p$

<0.001). The depletion in intracellular GSH by sulfasalazine was also observed in astrocytes. However, sulfasalazine only had a small effect on astrocytes (Figure 4C,  $p < 0.001$ ).

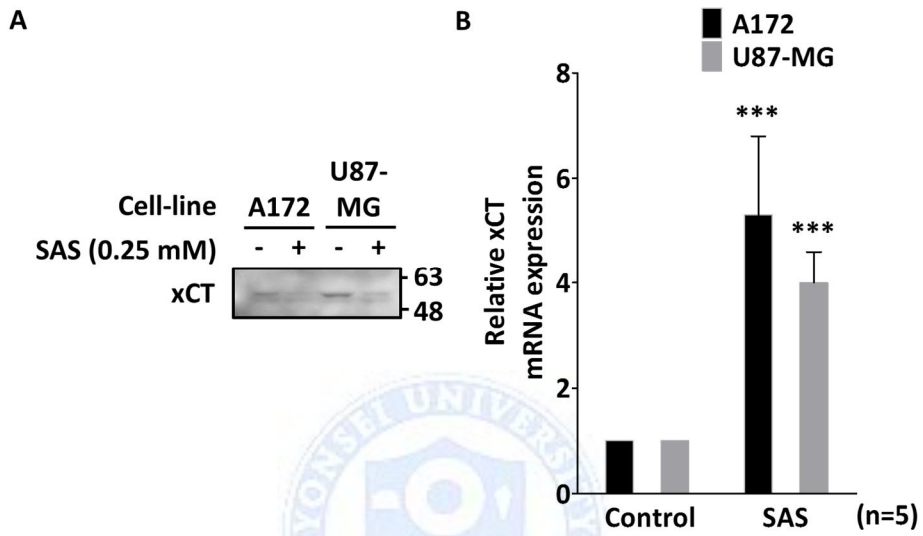


**Figure 3. System  $x_c^-$  inhibition by sulfasalazine (SAS) in glioblastoma and astrocytes.** (A) We performed the immune-blotting to evaluate the protein expression of xCT in GBM *in vitro*. After system  $x_c^-$  inhibition with SAS, the expression of xCT, the light chain of system  $x_c^-$ , was suppressed in A172 and U87-MG. (B) We performed the real-time PCR to investigate the change of xCT mRNA expression at 24 hours after the treatment of SAS (0.25mM) in GBM *in vitro*. xCT mRNA expression of SAS group was significantly elevated by the decrease of xCT protein expression compared to control (\*\*\* $p < 0.001$ ).

### (C) Dose determination using the cell viability assay

Cell viability assays were performed to determine the proper dose of sulfasalazine. The cell viability of A172 (Figure 5A,  $p = 0.082$ ) and U87-MG cells (Figure 5B,  $p = 0.171$ ) treated with 0.25 mM sulfasalazine was not significantly different from that of control cells. At 0.5 mM sulfasalazine was significantly more cytotoxic in both glioblastoma cell lines (A72 cells, Figure 5A,  $p < 0.001$ ); U87-MG cells, Figure 5B,  $p < 0.001$ ). Thus, a dose of 0.25 mM sulfasalazine was used to evaluate the radio-sensitizing effect of system  $x_c^-$  inhibition.

### B. Irradiation combined with system $x_c^-$ inhibition increased DSB compared to irradiation alone in glioblastoma *in vitro*

To evaluate whether the combination of irradiation with system  $x_c^-$  inhibition could elevate DNA damage, I performed the  $\gamma$ -H2AX focus formation assay to detect DNA damage. The induction of DNA DSB is followed by the formation of  $\gamma$ -H2AX foci, which are phosphorylated H2AX molecules in the chromatin flanking the DSB site. Twenty-four hours after treatment with 0.25 mM sulfasalazine, cells were irradiated with 2 and 10 Gy. The  $\gamma$ -H2AX was stained in green and the nucleus was stained in blue by DAPI (Figure 6A). Each  $\gamma$ -H2AX focus represents one radiation-induced DSB. Irradiation combined with sulfasalazine treatment induced a significant increase in  $\gamma$ -H2AX foci at each dose of irradiation in both glioblastoma cell lines (Figure 6A). I quantified the number of  $\gamma$ -H2AX foci per nucleus (Figure 6B and 6C). The combination of irradiation with sulfasalazine significantly increased the number of  $\gamma$ -H2AX foci

when compared to irradiation alone, regardless of the irradiation dose in both A172 (Figure 6B,  $p < 0.001$ ) and U87-MG cells (Figure 6C,  $p < 0.001$ ).

C. System  $x_c^-$  inhibition enhanced radio-sensitivity in glioblastoma *in vitro*

Next, I conducted clonogenic assays to evaluate the effects of system  $x_c^-$  inhibition on radio-sensitivity. The clonogenic cell survival assay, known as colony formation assay, determines the ability of a cell to proliferate indefinitely, thereby retaining its reproductive ability to form a large colony or a clone (Figure 7A). This cell is then considered clonogenic. The combination of irradiation and sulfasalazine treatment inhibited clonogenicity when compared to irradiation alone, when a 6 Gy irradiation was delivered (Figure 7A). In the irradiation plus sulfasalazine group, the surviving cell fraction was lower than that of the irradiation alone group at each dose in A172 cells (Figure 7B,  $p < 0.001$ ) and in U87-MG cells (Figure 7C,  $p < 0.001$ ).

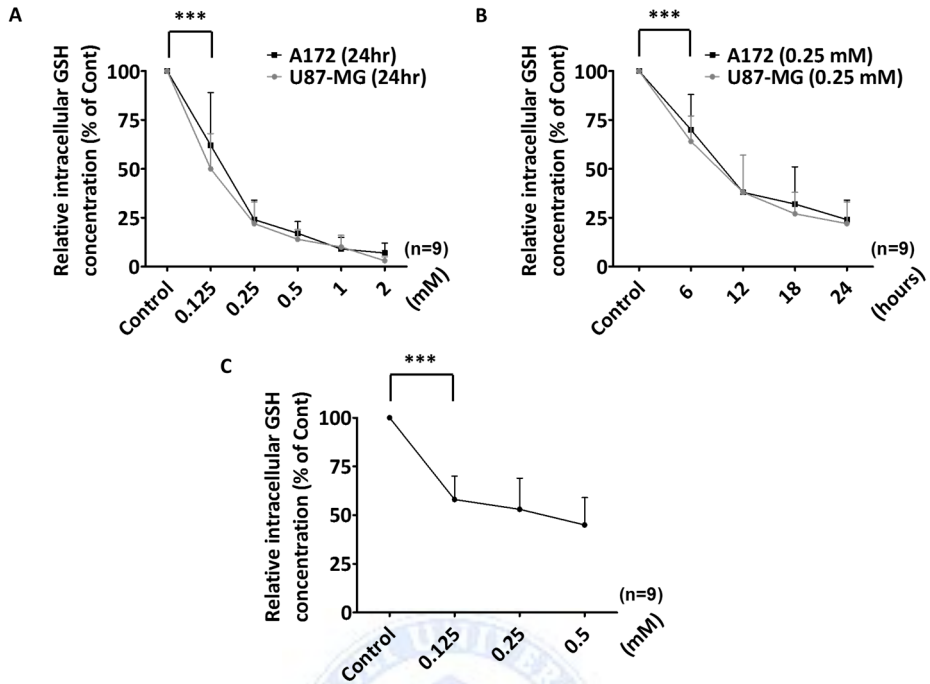


**Figure 4. Decrease in intracellular GSH induced by xCT inhibition in glioblastoma.** (A) and (B) We measured the intracellular GSH induced by system  $x_c^-$  inhibition. System  $x_c^-$  inhibition by sulfasalazine (SAS) causes a dose (A)- and time (B)- dependent reduction in GSH levels in A172 and U87-MG cells (\*\* $p < 0.001$ ). (C) Despite the depletion of intracellular GSH in astrocytes at 24 hours following SAS treatment, SAS only had a small effect on astrocytes (\*\* $p < 0.001$ ).

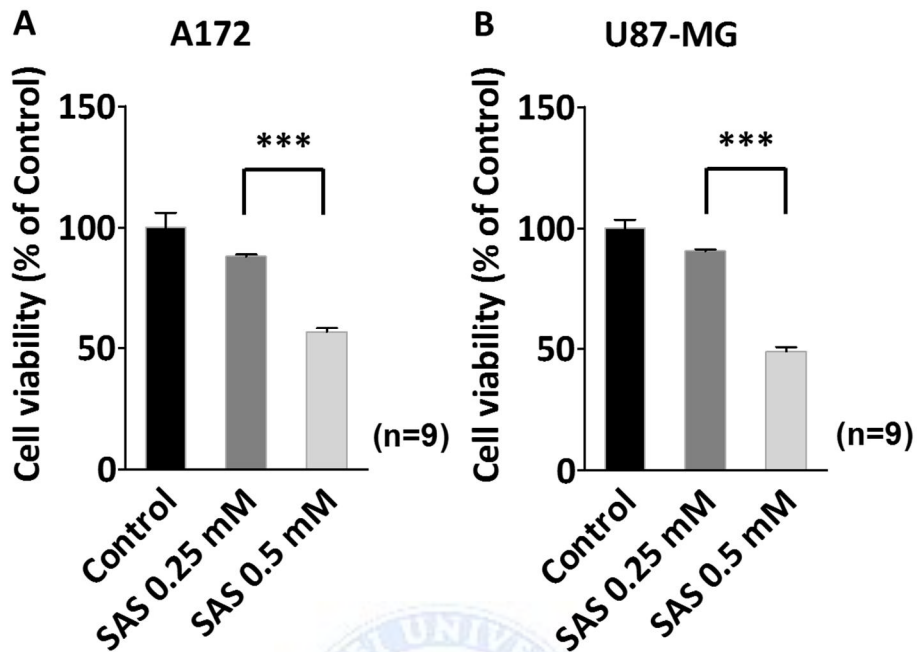


**Figure 5. Determination of the sulfasalazine (SAS) dose in A172 and U87-MG cells.** We performed the MTT assay to determine the proper dose of SAS based on cell viability. The cell viability of the cells treated with 0.25 mM SAS was not significantly different from that of the control in A172 (A) and U87-MG (B). However, 0.5 mM SAS was significantly more cytotoxic compared to control and 0.25 mM SAS in both cell lines (\*\**p* < 0.001).

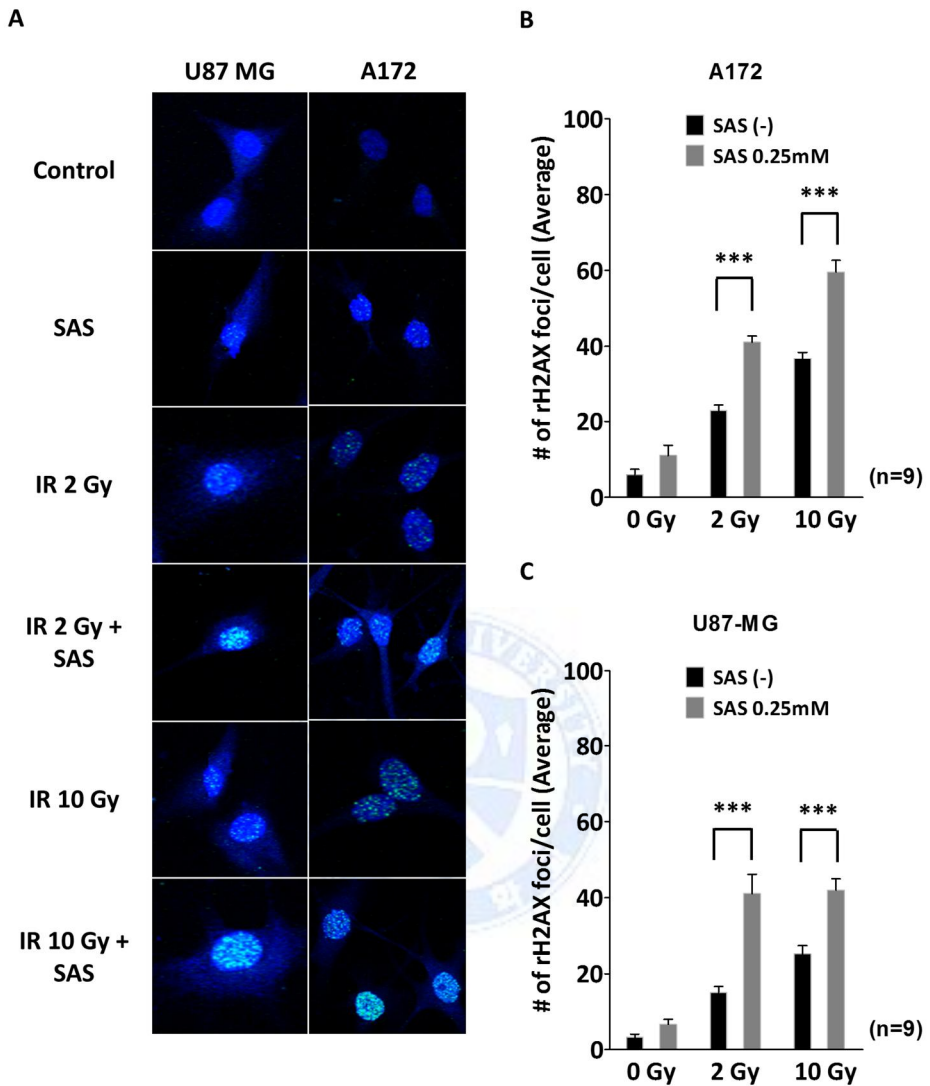


**Figure 6. The combination of irradiation with sulfasalazine (SAS) treatment increased DSB in glioblastoma.** The  $\gamma$ -H2AX foci formation assay was performed to evaluate the DNA DSB in each group. (A) Cells were irradiated with 2 and 10 Gy 24 hours following SAS (0.25 mM) treatment.  $\gamma$ -H2AX is stained in green and the nucleus is stained in blue by DAPI. Each  $\gamma$ -H2AX focus represents one radiation-induced DSB. (B) and (C) The combination of irradiation with SAS treatment significantly increased the number of  $\gamma$ -H2AX

foci compared to irradiation alone, regardless of the irradiation dose in both cell lines (\*\* $p < 0.001$  in both cell lines).

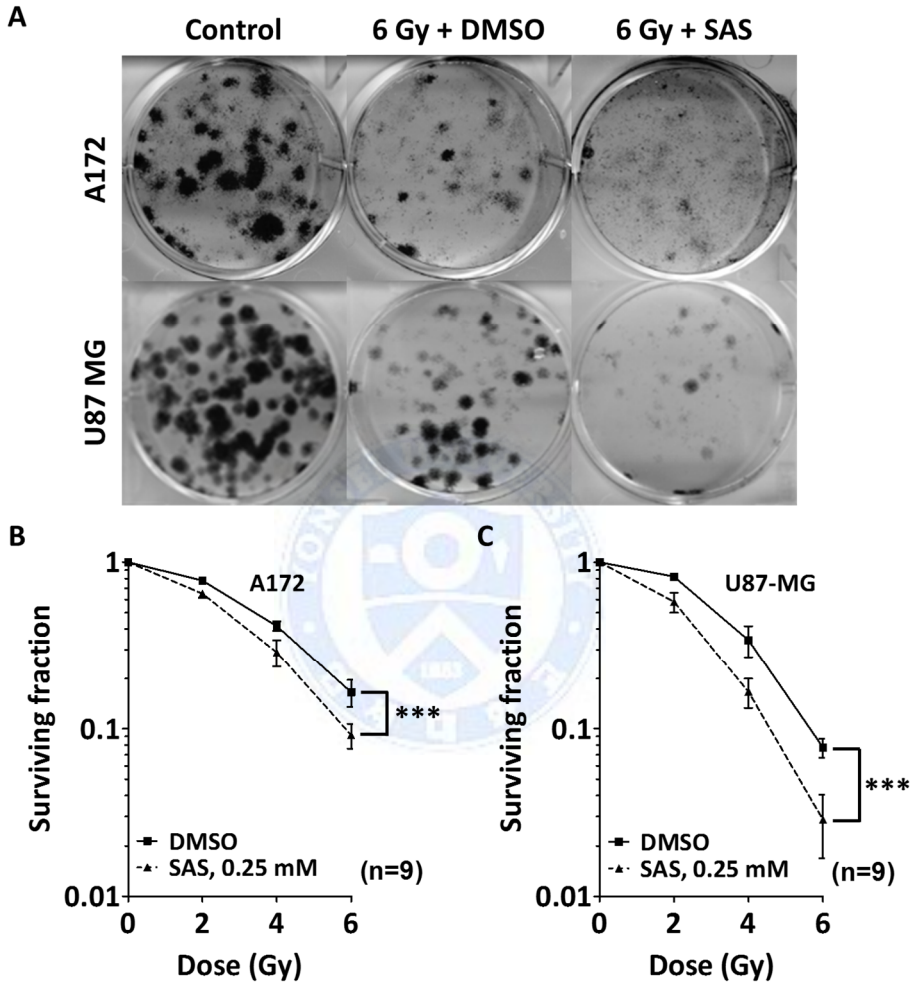


**Figure 7. System  $x_c^-$  inhibition enhanced radio-sensitivity in glioblastoma.** (A)

I performed the colony formation assay to investigate the radio-sensitivity according to the system  $x_c^-$  inhibition using A172 and U87-MG cells. (B) and (C) Survival curves based on colony formation assay. In the irradiation plus sulfasalazine group, the surviving cell fraction was lower than that of the

irradiation plus DMSO group at each dose in A172 (B) and U87-MG cells (C) (\*\* $p < 0.001$ ).

#### D. Summary

The combination of irradiation and inhibition of system  $x_c^-$  induced a significant increase in DSB and a significant decrease of the surviving cell fraction compared to irradiation alone in glioblastoma. In conclusion, my findings demonstrated that irradiation combined with system  $x_c^-$  inhibition could improve radio-sensitivity compared to irradiation alone in glioblastoma.



2. System  $x_c^-$  inhibition and cell migration through the change of mesenchymal markers

A. System  $x_c^-$  inhibition reduced the cell migration in glioblastoma *in vitro*

Wound healing (scratch) assay was conducted to investigate whether the combination of irradiation with sulfasalazine treatment could affect cell migration. In A172 and U87-MG cells, cells from the control and irradiation alone groups migrated more than cells from the sulfasalazine group with or without irradiation after 24 hours following the completion of irradiation (Figure 8A). Quantification of cell migration in both cell lines showed that the addition of sulfasalazine significantly prevented cell movement irrespectively of irradiation (Figure 8B and 8C,  $p < 0.001$  in both cell lines). Cell migration was significantly higher in the irradiation alone group than in the control group 24 hours following the completion of irradiation in both cell lines ( $p < 0.001$  in both cell lines). Despite the increase in migration induced by irradiation, the degree of inhibition of cell migration by sulfasalazine in the irradiation group was similar to that in the sulfasalazine alone group 24 hours after irradiation in both cell lines ( $p = 0.124$  in U87-MG and  $p > 0.99$  in A172).

To evaluate whether sulfasalazine cytotoxicity would affect the quantification of cell migration, I measured cell viability (Figure 9A and 9B). After 24 hours following the completion of irradiation in both cell lines, the rates of cell viability between all groups were not significantly different ( $p > 0.05$  in both cell lines).

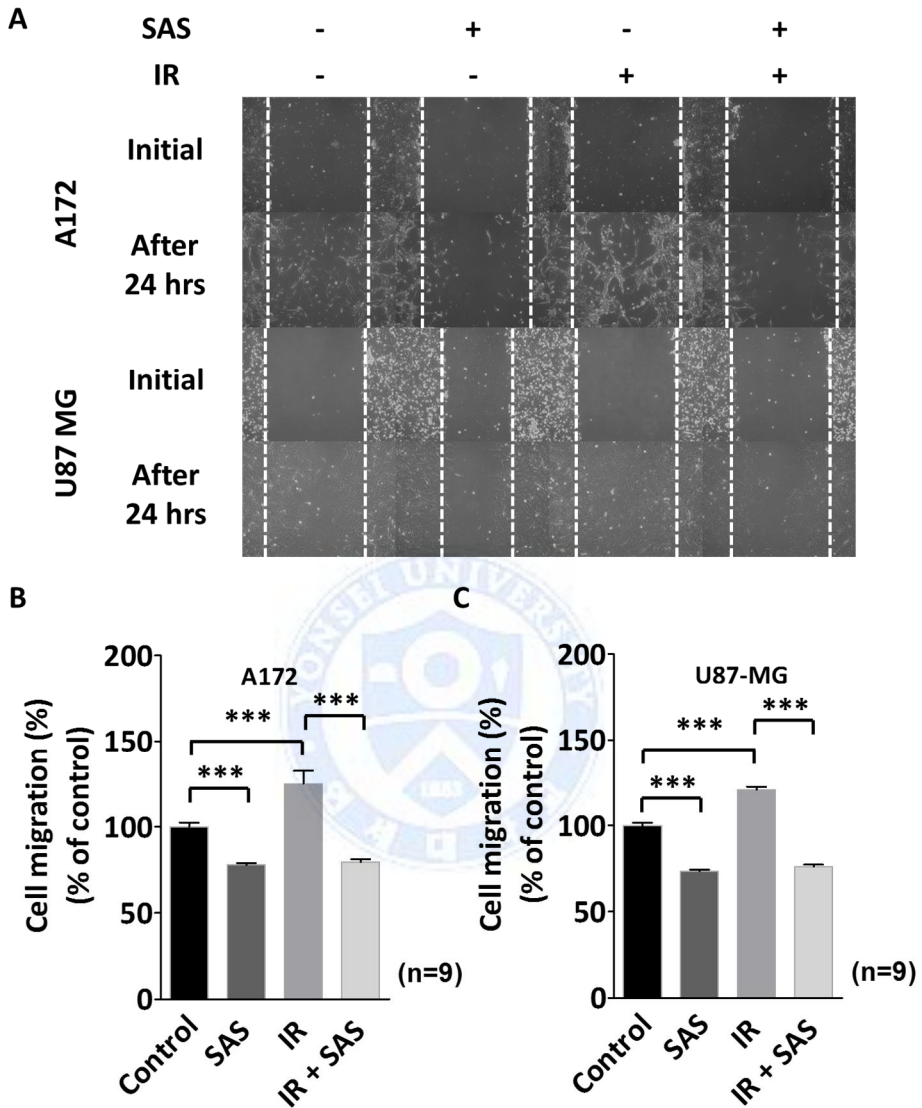


**Figure 8. System  $x_c^-$  inhibition reduced cell migration in glioblastoma. (A)**

We performed the wound healing assay to evaluate the cell migration. In both cell lines, cell migration was higher in the control and irradiation alone groups than in the sulfasalazine group with or without irradiation after 24 hours following the completion of irradiation. (B) and (C) Quantification of cell

migration in both cell lines showed that the addition of sulfasalazine significantly prevented cell movement irrespective of irradiation after 24 hours following the completion of irradiation (\*\* $p < 0.001$ ). Cell migration was significantly higher in the irradiation alone group than in the control group for both cell lines (††† $p < 0.001$ ). The degree of inhibition of cell migration by sulfasalazine in the irradiation group was similar to that of the sulfasalazine alone group ( $p > 0.99$  for A172 cells and  $p = 0.124$  for U87-MG cells).

B. System  $\chi_c^-$  inhibition decreased the expression levels of mesenchymal markers in glioblastoma *in vitro*

(A) IR increased the expression of the TCGA-based mesenchymal markers, CD44 and YKL-40 in glioblastoma *in vitro*

To evaluate whether irradiation could induce the mesenchymal transition, I evaluated the change in TCGA-based mesenchymal markers, CD44 and YKL-40, after irradiation. I performed RT-PCR using RNA from A172 and U87-MG cells after irradiation with 10 Gy. Irradiation significantly elevated *CD44* expression in A172 ( $p < 0.01$ ) and U87-MG cells ( $p < 0.05$ ) (Figure 10A) as well as *YKL-40* expression in both glioblastoma cell lines (Figure 10B,  $p < 0.05$  in both cell lines).

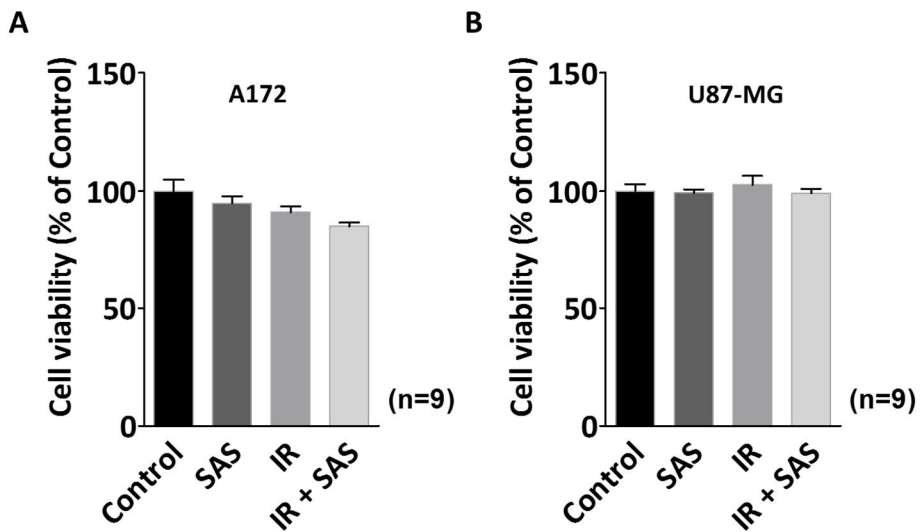


**Figure 9. Sulfasalazine cytotoxicity did not affect the cell migration.** (A) and (B) After 24 hours following the completion of irradiation in both cell lines, the rates of cell viability by sulfasalazine (SAS) between all groups were not significantly different ( $p > 0.05$  in both cell lines).

(B) System  $x_c^-$  inhibition decreased the mRNA expression of mesenchymal markers in glioblastoma *in vitro*

To investigate whether system  $x_c^-$  inhibition was associated with changes in mesenchymal markers in glioblastoma, I evaluated the mRNA expression of mesenchymal markers, *SNAIL*, vimentin, and N-cadherin. *SNAIL* mRNA expression in the irradiation group was significantly higher than that of the control group at 6 and 24 hours after irradiation in A172 cells (Figure 11A,  $p < 0.001$ ). However, *SNAIL* mRNA expression in the irradiation plus sulfasalazine group was significantly lower than that of the irradiation group (Figure 11A,  $p < 0.001$ ). Sulfasalazine alone also significantly decreased *SNAIL* mRNA level

compared to that of the control group (Figure 11A,  $p < 0.01$ ). Figure 11B depicts similar findings obtained in U87-MG cells. *SNAIL* mRNA expression was significantly higher in the irradiation group than in the control group at 6 and 24 hours after irradiation in U87-MG cell ( $p < 0.001$ ). *SNAIL* mRNA expression in the irradiation plus sulfasalazine group was significantly lower than that of the irradiation group ( $p < 0.001$ ). Sulfasalazine alone also significantly decreased *SNAIL* mRNA level when compared to that of the control group ( $p < 0.05$ ).

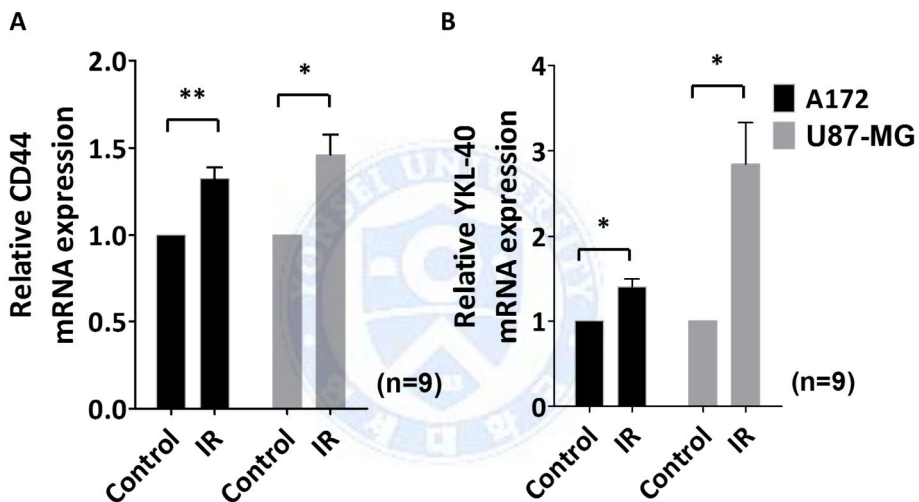


**Figure 10. Irradiation increased the expression of TCGA-based mesenchymal markers, CD44 and YKL-40.** We performed the real-time PCR to evaluate whether irradiation could increase the TCGA-based mesenchymal markers, CD44 and YKL-40, after irradiation. (A) Irradiation significantly elevated the expression of *CD44* in A172 (\*\* $p < 0.01$ ) and U87-MG cells (\* $p < 0.05$ ) compared to control. (B) Irradiation significantly increased YKL-40 expression in both glioblastoma cell lines (\* $p < 0.05$  in both cell lines) compared to control.

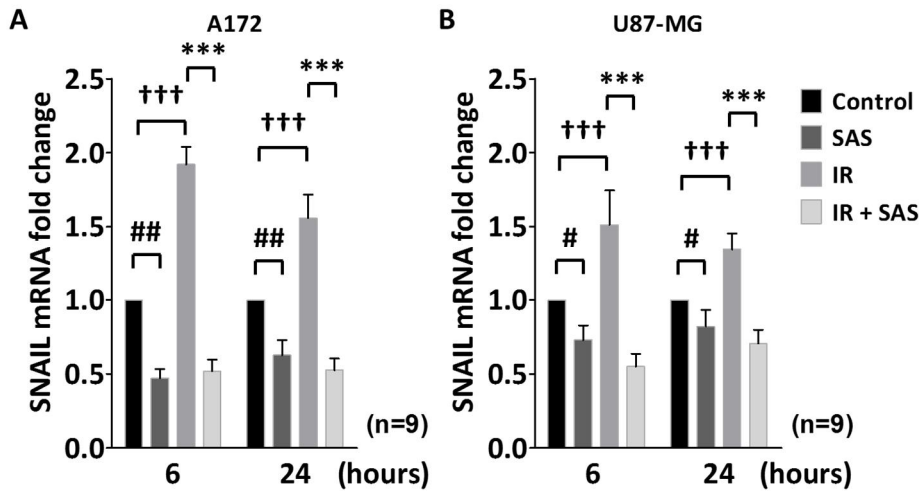


**Figure 11. System  $x_c^-$  inhibition decreased the *SNAIL* mRNA expression in glioblastoma.** We performed the real-time PCR to evaluate the mRNA expression of *SNAIL* (A) *SNAIL* mRNA expression in the irradiation group was significantly higher than that of the control group at 6 and 24 hours after irradiation in A172 cells ( $^{\dagger\dagger\dagger}p < 0.001$ ). However, *SNAIL* mRNA expression in the irradiation plus SAS group was significantly lower than that of the irradiation group ( $^{***}p < 0.001$ ). SAS alone also significantly decreased *SNAIL* mRNA level compared to that of the control group ( $^{##}p < 0.01$ ). (B) *SNAIL* mRNA expression was significantly higher in the irradiation group than in the control group at 6 and 24 hours after irradiation in U87-MG cell ( $^{\dagger\dagger\dagger}p < 0.001$ ). *SNAIL* mRNA expression in the irradiation plus SAS group was significantly lower than that of the irradiation group ( $^{***}p < 0.001$ ). SAS alone also significantly decreased *SNAIL* mRNA level compared to the control group ( $^{\#}p < 0.05$ ).

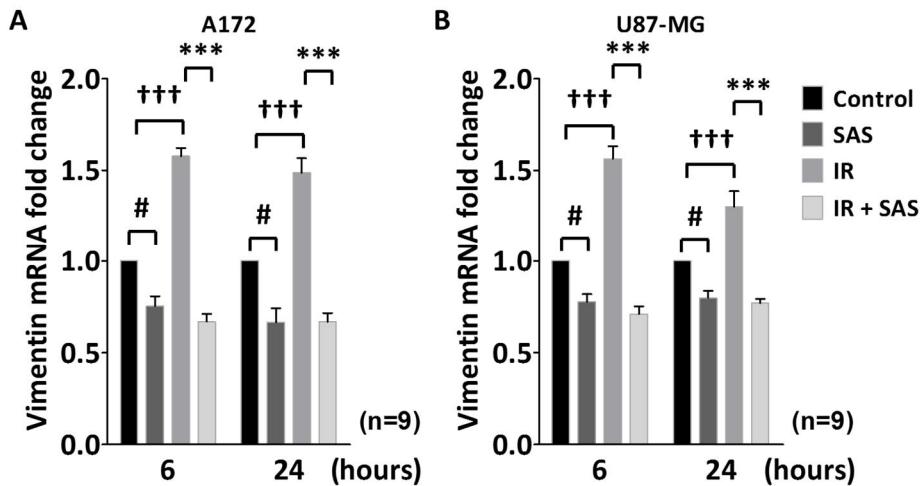


**Figure 12. System  $x_c^-$  inhibition decreased vimentin mRNA expression in glioblastoma.** We performed the real-time PCR to evaluate the mRNA expression of vimentin (A) Vimentin mRNA expression in the irradiation group was significantly higher than that of the control group at 6 and 24 hours after irradiation in A172 cells ( $†††p < 0.001$ ). However, vimentin mRNA expression in the irradiation plus SAS group was significantly lower than that of the irradiation group ( $***p < 0.001$ ). SAS alone also significantly decreased vimentin mRNA level compared to that of the control group ( $\#p < 0.05$ ). (B) Vimentin mRNA expression was significantly higher in the irradiation group than in the control group at 6 and 24 hours after irradiation in U87-MG cell ( $†††p < 0.001$ ). Vimentin mRNA expression in the irradiation plus SAS group was significantly lower than that of the irradiation group ( $***p < 0.001$ ). SAS alone also significantly decreased vimentin mRNA level compared to the control group ( $\#p < 0.05$ ).

Vimentin mRNA fold change was similar to that of *SNAIL* in both cell lines (Figure 12). My findings demonstrated that vimentin mRNA expression was significantly higher in the irradiation group than in the control group at 6

and 24 hours after irradiation in both glioblastoma (Figure 12A and 12B,  $p < 0.001$ ). However, vimentin mRNA expression was significantly lower in the irradiation plus sulfasalazine group than in the irradiation group (Figure 12A and 12B,  $p < 0.001$ ). Sulfasalazine alone also significantly decreased vimentin mRNA level when compared to the control group in both glioblastoma cell lines (Figure 12A and 12B,  $p < 0.05$ ).

N-cadherin mRNA expression was also significantly higher in the irradiation group than in the control group in both cell lines after 6 and 24 hours following the completion of irradiation (Figure 13A and 13B,  $p < 0.001$ ). The irradiation plus sulfasalazine group showed a significantly lower N-cadherin mRNA expression than the irradiation group in both cell lines (Figure 13A and 13B,  $p < 0.001$ ). However, N-cadherin mRNA expression was not significantly different between the sulfasalazine alone and the control groups in both cell lines, except for the significant difference at 24 hours after irradiation in U87-MG cells (Figure 13B,  $p < 0.01$ ).

There was no difference of alpha-SMA mRNA expression between all groups in A172 cells (Figure 14A). There was also no difference of alpha-SMA mRNA expression between all groups at 6 hours after irradiation in U87-MG cell (Figure 14B). However, alpha-SMA mRNA expression was significantly higher in the irradiation group than in the control group at 24 hours after irradiation (Figure 14B,  $p < 0.001$ ). Alpha-SMA mRNA expression in the irradiation plus SAS group was significantly lower than that of the irradiation group (Figure 14B,  $p < 0.01$ ). SAS alone significantly decreased alpha-SMA mRNA level compared to the control group at 24 hours after irradiation (Figure 14B,  $p < 0.01$ ).

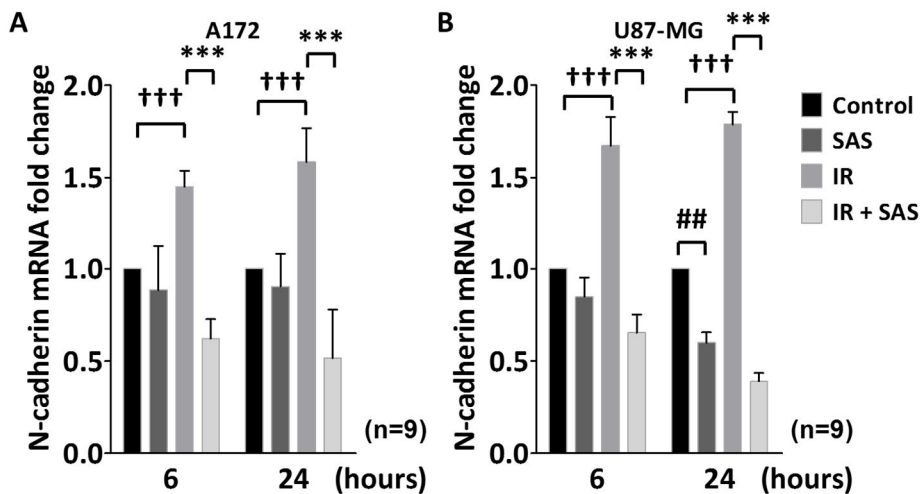


**Figure 13. System  $x_c^-$  inhibition decreased N-cadherin mRNA expression in glioblastoma.** We performed the real-time PCR to evaluate the mRNA expression of N-cadherin (A) N-cadherin mRNA expression in the irradiation group was significantly higher than that of the control group at 6 and 24 hours after irradiation in A172 cells ( $†††p < 0.001$ ). However, N-cadherin mRNA expression in the irradiation plus SAS group was significantly lower than that of the irradiation group ( $***p < 0.001$ ). (B) N-cadherin mRNA expression was significantly higher in the irradiation group than in the control group at 6 and 24 hours after irradiation in U87-MG cell ( $†††p < 0.001$ ). N-cadherin mRNA expression in the irradiation plus SAS group was significantly lower than that of the irradiation group ( $***p < 0.001$ ). SAS alone significantly decreased N-cadherin mRNA level compared to the control group at 24 hours after irradiation ( $##p < 0.05$ ).

Similar to alpha-SMA, there was no difference of FAP mRNA expression between all groups at 6 hours after irradiation in A172 cells. FAP mRNA expression was significantly higher in the irradiation group than in the control group at 24 hours after irradiation (Figure 15A,  $p < 0.05$ ). FAP mRNA expression in the irradiation plus SAS group was significantly lower than that of the irradiation group (Figure 15A,  $p = 0.01$ ). There was no difference of FAP mRNA expression between all groups at 6 hours after irradiation in U87-MG cell, similarly. Otherwise, FAP mRNA expression was significantly higher in the irradiation group than in the control group at 24 hours after irradiation (Figure 15B,  $p < 0.001$ ). FAP mRNA expression in the irradiation plus SAS group was significantly lower than that of the irradiation group (Figure 15B,  $p < 0.001$ ).

To evaluate whether sulfasalazine cytotoxicity would affect mRNA expression, I measured cell viability (Figure 16A and 16B). After 6 hours following the completion of irradiation in both cells, the rates of cell viability between all groups were not significantly different ( $p > 0.05$  in both cell lines).

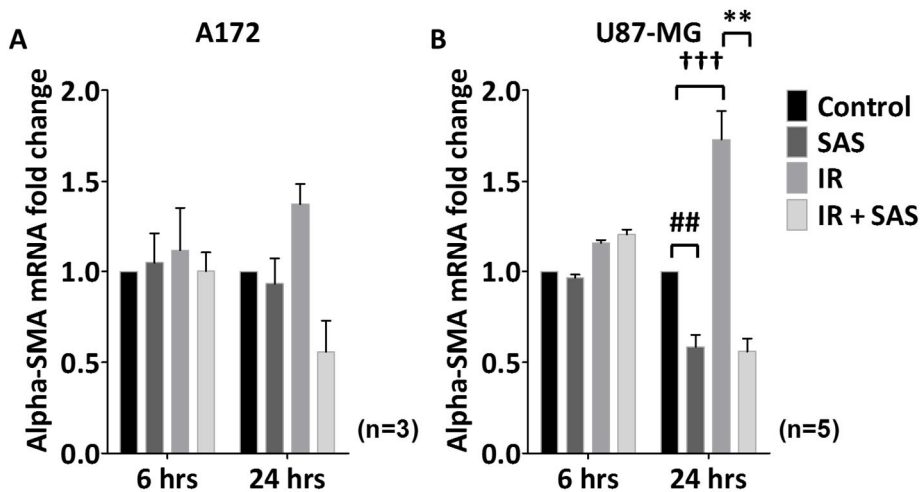


**Figure 14. System  $x_c^-$  inhibition decreased alpha-SMA mRNA expression in glioblastoma.** We performed the real-time PCR to evaluate the mRNA expression of alpha-SMA (A) There was no difference of alpha-SMA mRNA expression between all groups in A172 cells. (B) There was no difference of alpha-SMA mRNA expression between all groups at 6 hours after irradiation in U87-MG cell. Alpha-SMA mRNA expression was significantly higher in the irradiation group than in the control group at 24 hours after irradiation ( $^{+++}p < 0.001$ ). Alpha-SMA mRNA expression in the irradiation plus SAS group was significantly lower than that of the irradiation group ( $^{**}p < 0.01$ ). SAS alone significantly decreased alpha-SMA mRNA level compared to the control group at 24 hours after irradiation ( $^{##}p < 0.01$ ).

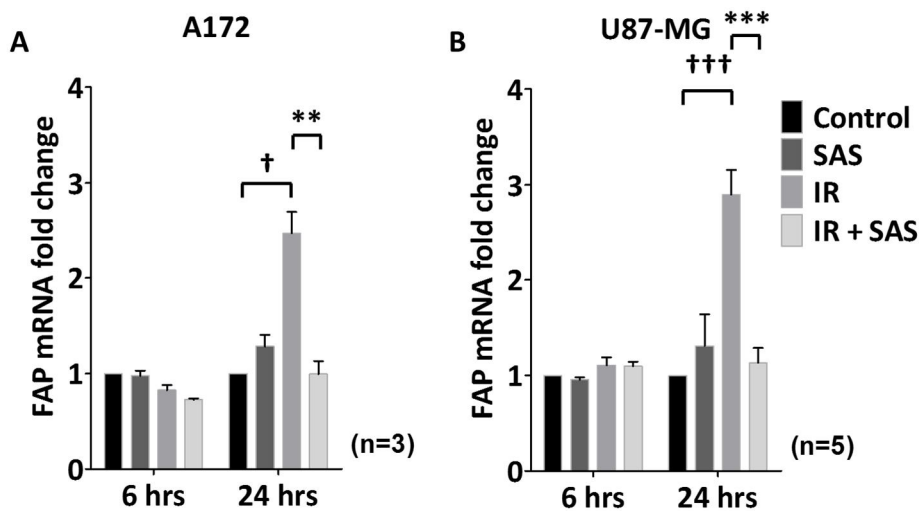


**Figure 15. System  $x_c^-$  inhibition decreased FAP mRNA expression in glioblastoma.** We performed the real-time PCR to evaluate the mRNA expression of FAP (A) There was no difference of FAP mRNA expression between all groups at 6 hours after irradiation in A172 cells. FAP mRNA expression was significantly higher in the irradiation group than in the control group at 24 hours after irradiation ( $^{\dagger}p < 0.05$ ). FAP mRNA expression in the irradiation plus SAS group was significantly lower than that of the irradiation group ( $^{**}p = 0.01$ ). (B) There was no difference of FAP mRNA expression between all groups at 6 hours after irradiation in U87-MG cell. FAP mRNA expression was significantly higher in the irradiation group than in the control group at 24 hours after irradiation ( $^{\dagger\dagger\dagger}p < 0.001$ ). FAP mRNA expression in the irradiation plus SAS group was significantly lower than that of the irradiation group ( $^{***}p < 0.001$ ).

(C) System  $x_c^-$  protein expression was higher in mesenchymal glioblastoma than in proneural glioblastoma

In addition, I investigated whether xCT protein expression level was related to the mesenchymal type of glioblastoma (Figure 17). I performed immunohistochemistry on human normal brain, and human proneural or mesenchymal glioblastoma tissues. xCT protein expression was observed by DAB staining. Hematoxylin was utilized for counterstaining. Normal brain tissue had a weak xCT protein expression. Similar to normal brain, one case of proneural glioblastoma presented a weak xCT protein expression, although xCT expression was induced by gliosis. However, three cases of mesenchymal glioblastoma showed a stronger xCT protein expression than cases of proneural glioblastoma.

### C. Summary

I observed that irradiation could induce the increase of mesenchymal markers in glioblastoma. My findings demonstrated that system  $x_c^-$  inhibition could reduce the irradiation-induced cell migration in glioblastoma. System  $x_c^-$  inhibition decreased mesenchymal markers in glioblastoma. System  $x_c^-$  protein expression was higher in mesenchymal glioblastoma specimens than in proneural glioblastoma and normal brain specimens.

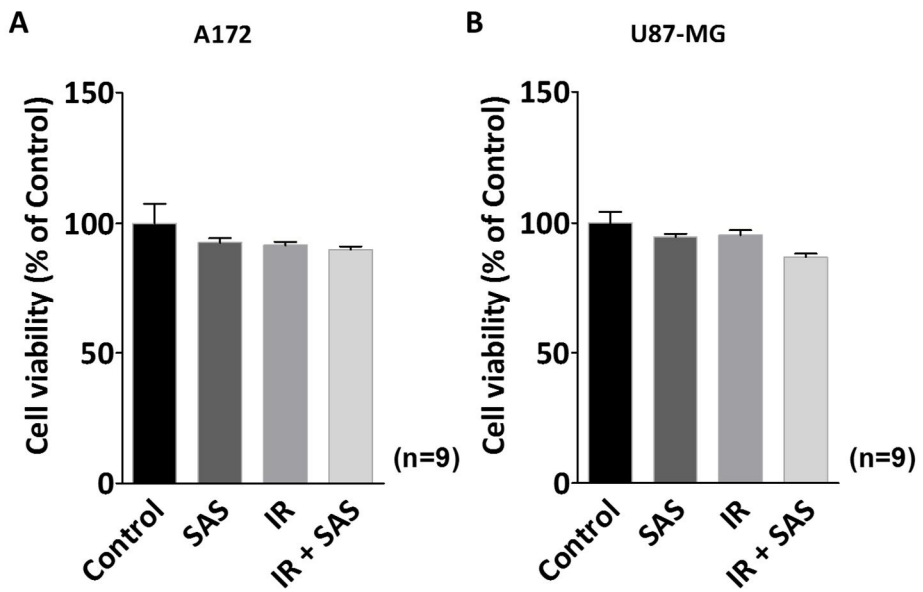


**Figure 16. Sulfasalazine cytotoxicity did not affect mRNA expression.** To evaluate whether sulfasalazine (SAS) cytotoxicity would affect mRNA expression, cell viability was measured in A172 and U87-MG cells (A and B).

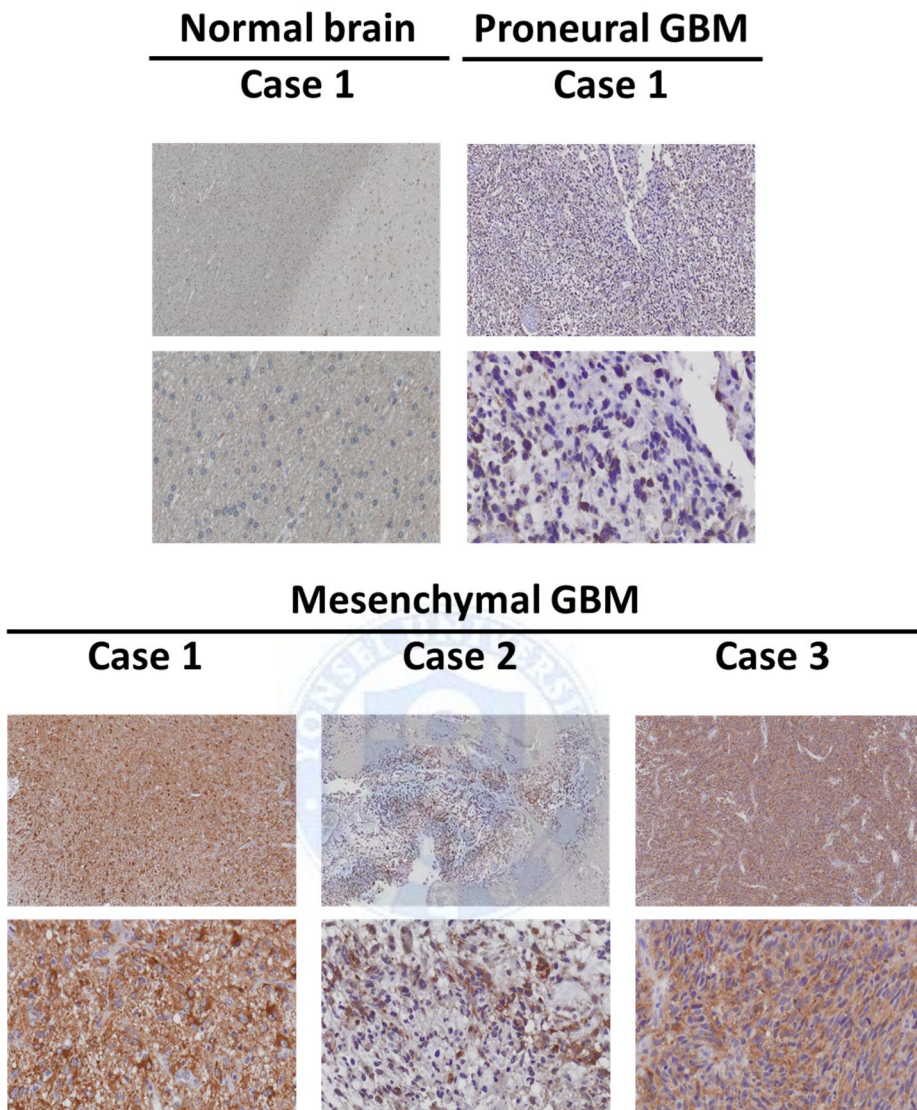


**Figure 17. The expression of system  $x_c^-$  protein was higher in mesenchymal glioblastoma than in proneural glioblastoma tissues.** Immunohistochemistry was performed on human normal brain, and human proneural or mesenchymal glioblastoma tissues. xCT expression was observed by DAB staining. Hematoxylin was utilized for counter staining. The upper and lower panels are images acquired at the 4× and 20× objectives, respectively. Normal brain tissue

showed a weak xCT expression. Similarly, specimens from patients with proneural glioblastoma presented a weak xCT protein expression, despite the mild elevation of xCT expression induced by gliosis. However, specimens from patients with mesenchymal glioblastoma presented a stronger xCT protein expression.



#### IV. DISCUSSION

This study demonstrated that system  $x_c^-$  inhibition can reduce intracellular cystine uptake and the resulting production of GSH. The combination of irradiation with system  $x_c^-$  inhibition significantly increased DSB and significantly decreased the surviving cell fraction compared to irradiation alone in glioblastoma. My findings showed that the combination of irradiation with system  $x_c^-$  inhibition enhances radio-sensitivity compared to irradiation alone in glioblastoma. My findings also demonstrated that irradiation induces cell migration through the changes in mesenchymal markers in glioblastoma. System  $x_c^-$  inhibition reduces the irradiation-induced cell migration in glioblastoma and decreases the expression of representative mesenchymal markers in glioblastoma. System  $x_c^-$  strong protein expression was significantly related to mesenchymal glioblastoma compared to proneural glioblastoma in human glioblastoma specimens.

My results indicate that system  $x_c^-$  inhibition by sulfasalazine reduces  $xCT$  protein expression and the intracellular uptake level of GSH in glioblastoma.  $xCT$  mRNA expression level increased after system  $x_c^-$  inhibition. I believe that this finding is linked to the appropriate inhibition of system  $x_c^-$  by sulfasalazine. However, there are two limitations to this conclusion. First, I did not directly analyze whether sulfasalazine could reduce the functional capacity of system  $x_c^-$ . In fact, I only determined the decrease of intracellular GSH level. However, previous studies on system  $x_c^-$  inhibition utilized sulfasalazine as a specific inhibitor of system  $x_c^-$ .<sup>25,26,28,31</sup> Furthermore, the finding that the intracellular level of GSH is reduced after sulfasalazine treatment supports and guarantees the inhibition of system  $x_c^-$  by sulfasalazine in most studies. Secondly, among several inhibitors of

system  $x_c^-$ , I only used sulfasalazine. Besides sulfasalazine, sulfapyridine, 5-aminosalicylic acid, S-(4)-CPG, and monosodium glutamate are xCT (SLC7A11) inhibitors as well. However, among them, sulfasalazine is the only drug currently used in the clinic for patients with inflammatory bowel diseases such as ulcerative colitis and Crohn's disease and rheumatoid arthritis.<sup>48-51</sup> Furthermore, 2 clinical studies validating the effect of sulfasalazine have been performed in glioma.<sup>52,53</sup> Robe *et al.* performed a phase I, II clinical trial for recurrent glioma. However, this trial failed to validate sulfasalazine effects for recurrent glioma, due to no treatment response and high rate of treatment-related toxicity, This was considered to result from the enrollment of patients with poor performance status.<sup>52</sup> Takeuchi *et al.* also reported no therapeutic benefit and high incidence of hematological side effects due to continuous administration over several weeks.<sup>53</sup> Although 2 clinical trials reported negative results, I believe that studies using sulfasalazine remain meaningful. Thus, this study was designed to determine the potential of sulfasalazine treatment. However, further studies are needed to determine the proper dose of sulfasalazine or to develop a new drug to inhibit system  $x_c^-$  in patients with glioblastoma.

This study showed that xCT inhibition induced a dose- and time-dependent reduction of intracellular GSH in glioblastoma. In astrocytes, xCT inhibition by sulfasalazine reduced the intracellular GSH level in a dose- and time-dependent manner. However, sulfasalazine had only a small effect on astrocytes. Normally, the sodium-independent system  $x_c^-$  is mainly expressed on astrocytes and is the main route of cystine uptake and production of intracellular GSH in these cells.<sup>54</sup> Glutamate released from astrocytes could be taken up by adjacent neurons to regulate synaptic function.<sup>55,56</sup> If glutamate is released immoderately from

astrocytes, it could result in the neuro-excitotoxicity. The system  $x_c^-$  mediates the interaction between astrocytes and neurons. Thus, I believe that  $xCT$  inhibition may decrease the intracellular level of GSH in astrocytes. In this study,  $xCT$  protein expression level in the normal brain, including glial cells, was significantly lower than that in human glioblastoma tissues. I think that this finding can explain why the degree of reduction in GSH levels in astrocytes is significantly lower than that in glioblastoma. Chung *et al.* demonstrated similar findings.<sup>9</sup> They also depicted that sulfasalazine caused a time- and dose-dependent decrease in intracellular GSH in D54-MG glioblastoma. However, the effect of sulfasalazine treatment was significantly lower on intracellular levels of GSH in astrocytes.

I determined that sulfasalazine should be used at a dose of 0.25 mM based on cell viability assay. Previous studies used 0.5 mM sulfasalazine to inhibit  $xCT$  in most experiments.<sup>9,25</sup> These studies investigated whether system  $x_c^-$  inhibition alone could prevent cancer progression and growth. In this study, I evaluated whether system  $x_c^-$  inhibition combined with irradiation could enhance radio-sensitivity compared to irradiation alone in glioblastoma. Thus, I needed to exclude the possibility that sulfasalazine alone had cytotoxic effects. My findings demonstrated that 0.5 mM sulfasalazine was significantly more cytotoxic than control and 0.25 mM sulfasalazine. Furthermore, 24 hours after treatment with 0.25 mM sulfasalazine, the decrease in the relative intracellular GSH levels was less than 75% when compared to the control group in A172 and U87-MG glioblastoma. Based on my findings about enhanced radio-sensitivity, I consider that 0.25 mM of sulfasalazine would be the proper dose to investigate whether system  $x_c^-$  inhibition is related to enhanced radio-sensitivity.

In this study, irradiation with the xCT inhibition increased DNA DSB compared to irradiation alone in glioblastoma as observed using the  $\gamma$ -H2AX focus formation assay. Similar to my findings, Sleire *et al.* recently reported that 1 mM sulfasalazine and irradiation synergistically increase DNA damage in glioma cells by measuring  $\gamma$ -H2AX focus formation.<sup>57</sup> However, my findings are different because irradiation with 0.25 mM sulfasalazine did not increase DNA damage when compared to the radiation only group. Comparing their method to mine, they performed the  $\gamma$ -H2AX focus assay 15 minutes after an 8 Gy irradiation, while I performed the  $\gamma$ -H2AX focus assay 24 hours after the completion of 2 Gy and 10 Gy irradiations. This discrepancy may explain the differences observed in term of  $\gamma$ -H2AX focus assay.

Furthermore, the clonogenic assay indicated that the surviving cell fraction of the irradiation plus sulfasalazine group was lower than that of the irradiation alone group at each dose. This method is traditionally used to test radio-sensitivity, because it measures the ability of individual cells to proliferate indefinitely. This assay allows us to determine the number of colonies formed from known numbers of cells, providing us with the percentage of cell survival as a function of the irradiation dose. The cell viability assay is also used to evaluate radio-sensitivity.<sup>58</sup> It measures cell growth based on enzyme activity in viable cells. Live cells, presenting higher enzyme activity, transform the dye, resulting in a higher absorbance at a specific wavelength, which is directly correlated to the number of live cells. The cell viability assay is more rapid and less laborious than the clonogenic assay. However, the cell viability assay does not allow the measurement of indefinite proliferation. To validate itself, the cell viability assay should be compared to the clonogenic assay. In this study, my data from the clonogenic assay

validated that system  $x_c^-$  inhibition enhances radio-sensitivity. Sleire *et al.* also demonstrated that sulfasalazine and irradiation synergistically increase glioma cell death using the MTS viability assay.<sup>57</sup> They demonstrated that cells treated with 0.25 mM sulfasalazine combined with irradiation showed lower cell viability compared to cells not treated with sulfasalazine, despite of a difference of DNA damage between 0.25 mM sulfasalazine and combination of 0.25 mM sulfasalazine with irradiation. Thus, I consider that combining 0.25 mM sulfasalazine with irradiation could substantially enhance radio-sensitivity in glioblastoma.

I found that irradiation enhances cell migration through the increase of mesenchymal markers and system  $x_c^-$  inhibition reduces irradiation-induced cell migration through the increase of mesenchymal markers. Many studies also demonstrated radiation-induced EMT in various epithelial cancers, and radiation-induced glial-mesenchymal transition in glioblastoma *in vitro*.<sup>40-42,59,60</sup> Irradiation-induced EMT is known to be activated by nuclear factor kappa-light-chain-enhancer of activated B cells (NF- $\kappa$ B) or transforming growth factor beta (TGF- $\beta$ ).<sup>59,60</sup> Irradiation induces NF- $\kappa$ B activation.<sup>61</sup> Furthermore, ROS induces EMT, which is mediated by NF- $\kappa$ B-dependent activation of SNAIL.<sup>62,63</sup> Recently, Bhat *et al.* demonstrated that mesenchymal differentiation mediated by NF- $\kappa$ B promotes radiation resistance in glioblastoma.<sup>64</sup> Irradiation induces the TGF- $\beta$  signaling pathway.<sup>65</sup> Recently, Mahabir *et al.* demonstrated that sustained elevation of SNAIL promotes glial-mesenchymal transition after irradiation in malignant glioma.<sup>42</sup> They showed that the expression of the mesenchymal markers vimentin, CD44, and YKL-40, increased in clinically recurrent malignant glioma. Additionally, irradiation increased CD44 and YKL-40 expression in glioblastoma and induced the glial-mesenchymal transition. Thus, I believe that the increase in ROS induced by

the combination of irradiation with system  $\chi_c^-$  inhibition could promote the mesenchymal transition through either NF- $\kappa$ B or TGF- $\beta$ , which could result in radio-resistance and treatment-failure. However, using the wound healing assay, I found that the combination of sulfasalazine with irradiation reduced cell migration and the expression of mesenchymal markers such as vimentin, N-cadherin, SNAIL, alpha-SMA and FAP when compared to the irradiation only group. Therefore, I consider that the combination of system  $\chi_c^-$  inhibition and irradiation could enhance local therapeutic effects by improving radio-sensitivity and concurrently reducing migration and invasion of glioblastoma through inhibition of the increase of mesenchymal markers.

Thus, I investigated whether xCT protein expression level was related to the mesenchymal type of glioblastoma in human tissues by immunohistochemistry. I observed that the xCT protein expression was significantly higher in mesenchymal than in proneural human glioblastoma specimens. Several studies showed that xCT protein expression is significantly stronger in tumors than in normal brain tissues.<sup>8,57</sup> However, no study demonstrated differences in xCT protein expression based on genomic subtypes of glioblastoma. This study is the first to describe a difference in xCT protein expression based on genomic subtypes of glioblastoma. Furthermore, because the mesenchymal glioblastoma is known to have the worst prognosis among the genomic subtypes of glioblastoma, I consider that this points could imply the clinical availability of combination therapy of system  $\chi_c^-$  inhibition and RT in primary or recurrent mesenchymal glioblastoma. Although further clinical trials to investigate the survival benefit of combination therapy of system  $\chi_c^-$  inhibition and RT in mesenchymal glioblastoma patients, I suggest that my study open up the exciting prospects to improve the survival in mesenchymal glioblastoma.

#### IV. CONCLUSION

In conclusion, my findings demonstrate that system  $x_c^-$  inhibition in combination with irradiation increased DNA damage and enhance radio-sensitivity in glioblastoma. Furthermore, system  $x_c^-$  inhibition prevented the IR-induced cell migration and affected mesenchymal features in glioblastoma. I believe that the combination of RT and system  $x_c^-$  inhibition could help improve glioblastoma therapeutic outcome.



## REFERENCES

1. Lewerenz J, Maher P, Methner A. Regulation of xCT expression and system x (c) (-) function in neuronal cells. *Amino Acids* 2012;42:171-9.
2. Robert SM, Ogunrinu-Babarinde T, Holt KT, Sontheimer H. Role of glutamate transporters in redox homeostasis of the brain. *Neurochem Int* 2014;73:181-91.
3. Dringen R. Metabolism and functions of glutathione in brain. *Prog Neurobiol* 2000;62:649-71.
4. McBean GJ. Cerebral cystine uptake: a tale of two transporters. *Trends Pharmacol Sci* 2002;23:299-302.
5. Bannai S. Exchange of cystine and glutamate across plasma membrane of human fibroblasts. *J Biol Chem* 1986;261:2256-63.
6. Vene R, Castellani P, Delfino L, Lucibello M, Ciriolo MR, Rubartelli A. The cystine/cysteine cycle and GSH are independent and crucial antioxidant systems in malignant melanoma cells and represent druggable targets. *Antioxid Redox Signal* 2011;15:2439-53.
7. Banjac A, Perisic T, Sato H, Seiler A, Bannai S, Weiss N, et al. The cystine/cysteine cycle: a redox cycle regulating susceptibility versus resistance to cell death. *Oncogene* 2008;27:1618-28.
8. Takeuchi S, Wada K, Toyooka T, Shinomiya N, Shimazaki H, Nakanishi K, et al. Increased xCT expression correlates with tumor invasion and outcome in patients with glioblastomas. *Neurosurgery* 2013;72:33-41; discussion
9. Chung WJ, Lyons SA, Nelson GM, Hamza H, Gladson CL, Gillespie GY, et al. Inhibition of cystine uptake disrupts the growth of primary brain tumors. *J Neurosci* 2005;25:7101-10.
10. Sontheimer H. A role for glutamate in growth and invasion of primary brain tumors. *J Neurochem* 2008;105:287-95.

11. de Groot J, Sontheimer H. Glutamate and the biology of gliomas. *Glia* 2011;59:1181-9.
12. Porter KR, McCarthy BJ, Freels S, Kim Y, Davis FG. Prevalence estimates for primary brain tumors in the United States by age, gender, behavior, and histology. *Neuro Oncol* 2010;12:520-7.
13. Dolecek TA, Propp JM, Stroup NE, Kruchko C. CBTRUS statistical report: primary brain and central nervous system tumors diagnosed in the United States in 2005-2009. *Neuro Oncol* 2012;14 Suppl 5:v1-49.
14. Louis DN, Ohgaki H, Wiestler OD, Cavenee WK, Burger PC, Jouvet A, et al. The 2007 WHO classification of tumours of the central nervous system. *Acta Neuropathol* 2007;114:97-109.
15. Stupp R, Mason WP, van den Bent MJ, Weller M, Fisher B, Taphoorn MJ, et al. Radiotherapy plus concomitant and adjuvant temozolomide for glioblastoma. *N Engl J Med* 2005;352:987-96.
16. Omuro A, DeAngelis LM. Glioblastoma and other malignant gliomas: a clinical review. *JAMA* 2013;310:1842-50.
17. Dunn GP, Rinne ML, Wykosky J, Genovese G, Quayle SN, Dunn IF, et al. Emerging insights into the molecular and cellular basis of glioblastoma. *Genes Dev* 2012;26:756-84.
18. Bao S, Wu Q, McLendon RE, Hao Y, Shi Q, Hjelmeland AB, et al. Glioma stem cells promote radioresistance by preferential activation of the DNA damage response. *Nature* 2006;444:756-60.
19. Li Z, Wang H, Eyler CE, Hjelmeland AB, Rich JN. Turning cancer stem cells inside out: an exploration of glioma stem cell signaling pathways. *J Biol Chem* 2009;284:16705-9.
20. De Bont R, van Larebeke N. Endogenous DNA damage in humans: a review of quantitative data. *Mutagenesis* 2004;19:169-85.
21. Jackson SP, Bartek J. The DNA-damage response in human biology and disease. *Nature* 2009;461:1071-8.

22. El-Gebali S, Bentz S, Hediger MA, Anderle P. Solute carriers (SLCs) in cancer. *Mol Aspects Med* 2013;34:719-34.
23. Ishii T, Mann GE. Redox status in mammalian cells and stem cells during culture in vitro: critical roles of Nrf2 and cystine transporter activity in the maintenance of redox balance. *Redox Biol* 2014;2:786-94.
24. Trachootham D, Alexandre J, Huang P. Targeting cancer cells by ROS-mediated mechanisms: a radical therapeutic approach? *Nat Rev Drug Discov* 2009;8:579-91.
25. Ishimoto T, Nagano O, Yae T, Tamada M, Motohara T, Oshima H, et al. CD44 variant regulates redox status in cancer cells by stabilizing the xCT subunit of system xc(-) and thereby promotes tumor growth. *Cancer Cell* 2011;19:387-400.
26. Chen RS, Song YM, Zhou ZY, Tong T, Li Y, Fu M, et al. Disruption of xCT inhibits cancer cell metastasis via the caveolin-1/beta-catenin pathway. *Oncogene* 2009;28:599-609.
27. Mima K, Okabe H, Ishimoto T, Hayashi H, Nakagawa S, Kuroki H, et al. CD44s regulates the TGF-beta-mediated mesenchymal phenotype and is associated with poor prognosis in patients with hepatocellular carcinoma. *Cancer Res* 2012;72:3414-23.
28. Yoshikawa M, Tsuchihashi K, Ishimoto T, Yae T, Motohara T, Sugihara E, et al. xCT inhibition depletes CD44v-expressing tumor cells that are resistant to EGFR-targeted therapy in head and neck squamous cell carcinoma. *Cancer Res* 2013;73:1855-66.
29. Lo M, Wang YZ, Gout PW. The x(c)- cystine/glutamate antiporter: a potential target for therapy of cancer and other diseases. *J Cell Physiol* 2008;215:593-602.
30. Lo M, Ling V, Wang YZ, Gout PW. The xc- cystine/glutamate antiporter: a mediator of pancreatic cancer growth with a role in drug resistance. *Br J Cancer* 2008;99:464-72.

31. Guan J, Lo M, Dockery P, Mahon S, Karp CM, Buckley AR, et al. The xc-cystine/glutamate antiporter as a potential therapeutic target for small-cell lung cancer: use of sulfasalazine. *Cancer Chemother Pharmacol* 2009;64:463-72.
32. Allalunis-Turner MJ, Day RS, 3rd, McKean JD, Petruk KC, Allen PB, Aronyk KE, et al. Glutathione levels and chemosensitizing effects of buthionine sulfoximine in human malignant glioma cells. *J Neurooncol* 1991;11:157-64.
33. Singer E, Judkins J, Salomonis N, Matlaf L, Soteropoulos P, McAllister S, et al. Reactive oxygen species-mediated therapeutic response and resistance in glioblastoma. *Cell Death Dis* 2015;6:e1601.
34. Ye ZC, Rothstein JD, Sontheimer H. Compromised glutamate transport in human glioma cells: reduction-mislocalization of sodium-dependent glutamate transporters and enhanced activity of cystine-glutamate exchange. *J Neurosci* 1999;19:10767-77.
35. Schunemann DP, Grivicich I, Regner A, Leal LF, de Araujo DR, Jotz GP, et al. Glutamate promotes cell growth by EGFR signaling on U-87MG human glioblastoma cell line. *Pathol Oncol Res* 2010;16:285-93.
36. Takano T, Lin JH, Arcuino G, Gao Q, Yang J, Nedergaard M. Glutamate release promotes growth of malignant gliomas. *Nat Med* 2001;7:1010-5.
37. Verhaak RG, Hoadley KA, Purdom E, Wang V, Qi Y, Wilkerson MD, et al. Integrated genomic analysis identifies clinically relevant subtypes of glioblastoma characterized by abnormalities in PDGFRA, IDH1, EGFR, and NF1. *Cancer Cell* 2010;17:98-110.
38. Phillips HS, Kharbanda S, Chen R, Forrest WF, Soriano RH, Wu TD, et al. Molecular subclasses of high-grade glioma predict prognosis, delineate a pattern of disease progression, and resemble stages in neurogenesis. *Cancer Cell* 2006;9:157-73.

39. Lee Y, Scheck AC, Cloughesy TF, Lai A, Dong J, Farooqi HK, et al. Gene expression analysis of glioblastomas identifies the major molecular basis for the prognostic benefit of younger age. *BMC Med Genomics* 2008;1:52.
40. Jung JW, Hwang SY, Hwang JS, Oh ES, Park S, Han IO. Ionising radiation induces changes associated with epithelial-mesenchymal transdifferentiation and increased cell motility of A549 lung epithelial cells. *Eur J Cancer* 2007;43:1214-24.
41. Kawamoto A, Yokoe T, Tanaka K, Saigusa S, Toiyama Y, Yasuda H, et al. Radiation induces epithelial-mesenchymal transition in colorectal cancer cells. *Oncol Rep* 2012;27:51-7.
42. Mahabir R, Tanino M, Elmansuri A, Wang L, Kimura T, Itoh T, et al. Sustained elevation of Snail promotes glial-mesenchymal transition after irradiation in malignant glioma. *Neuro Oncol* 2014;16:671-85.
43. Choi DW, Maulucci-Gedde M, Kriegstein AR. Glutamate neurotoxicity in cortical cell culture. *J Neurosci* 1987;7:357-68.
44. Ko SJ, Isozaki K, Kim I, Lee JH, Cho HJ, Sohn SY, et al. PKC phosphorylation regulates mGluR5 trafficking by enhancing binding of Siah-1A. *J Neurosci* 2012;32:16391-401.
45. Franken NA, Rodermond HM, Stap J, Haveman J, van Bree C. Clonogenic assay of cells in vitro. *Nat Protoc* 2006;1:2315-9.
46. Kim YB, Jeung HC, Jeong I, Lee K, Rha SY, Chung HC, et al. Mechanism of enhancement of radiation-induced cytotoxicity by sorafenib in colorectal cancer. *J Radiat Res* 2013;54:52-60.
47. Liang CC, Park AY, Guan JL. In vitro scratch assay: a convenient and inexpensive method for analysis of cell migration in vitro. *Nat Protoc* 2007;2:329-33.
48. Ordas I, Eckmann L, Talamini M, Baumgart DC, Sandborn WJ. Ulcerative colitis. *Lancet* 2012;380:1606-19.

49. Jansen G, van der Heijden J, Oerlemans R, Lems WF, Ifergan I, Scheper RJ, et al. Sulfasalazine is a potent inhibitor of the reduced folate carrier: implications for combination therapies with methotrexate in rheumatoid arthritis. *Arthritis Rheum* 2004;50:2130-9.
50. Steiman AJ, Pope JE, Thiessen-Philbrook H, Li L, Barnabe C, Kalache F, et al. Non-biologic disease-modifying antirheumatic drugs (DMARDs) improve pain in inflammatory arthritis (IA): a systematic literature review of randomized controlled trials. *Rheumatol Int* 2013;33:1105-20.
51. Gout PW, Buckley AR, Simms CR, Bruchovsky N. Sulfasalazine, a potent suppressor of lymphoma growth by inhibition of the x(c)- cystine transporter: a new action for an old drug. *Leukemia* 2001;15:1633-40.
52. Robe PA, Martin DH, Nguyen-Khac MT, Artesi M, Deprez M, Albert A, et al. Early termination of ISRCTN45828668, a phase 1/2 prospective, randomized study of sulfasalazine for the treatment of progressing malignant gliomas in adults. *BMC Cancer* 2009;9:372.
53. Takeuchi S, Wada K, Nagatani K, Otani N, Osada H, Nawashiro H. Sulfasalazine and temozolomide with radiation therapy for newly diagnosed glioblastoma. *Neurol India* 2014;62:42-7.
54. Lobner D. Mechanisms of beta-N-methylamino-L-alanine induced neurotoxicity. *Amyotroph Lateral Scler* 2009;10 Suppl 2:56-60.
55. Xi ZX, Ramamoorthy S, Baker DA, Shen H, Samuvel DJ, Kalivas PW. Modulation of group II metabotropic glutamate receptor signaling by chronic cocaine. *J Pharmacol Exp Ther* 2002;303:608-15.
56. Baker DA, Xi ZX, Shen H, Swanson CJ, Kalivas PW. The origin and neuronal function of in vivo nonsynaptic glutamate. *J Neurosci* 2002;22:9134-41.
57. Sleire L, Skeie BS, Netland IA, Forde HE, Dodoo E, Selheim F, et al. Drug repurposing: sulfasalazine sensitizes gliomas to gamma knife radiosurgery

- by blocking cystine uptake through system Xc, leading to glutathione depletion. *Oncogene* 2015.
58. Vichai V, Kirtikara K. Sulforhodamine B colorimetric assay for cytotoxicity screening. *Nat Protoc* 2006;1:1112-6.
  59. Zhou YC, Liu JY, Li J, Zhang J, Xu YQ, Zhang HW, et al. Ionizing radiation promotes migration and invasion of cancer cells through transforming growth factor-beta-mediated epithelial-mesenchymal transition. *Int J Radiat Oncol Biol Phys* 2011;81:1530-7.
  60. Yan S, Wang Y, Yang Q, Li X, Kong X, Zhang N, et al. Low-dose radiation-induced epithelial-mesenchymal transition through NF-kappaB in cervical cancer cells. *Int J Oncol* 2013;42:1801-6.
  61. Lee SJ, Dimtchev A, Lavin MF, Dritschilo A, Jung M. A novel ionizing radiation-induced signaling pathway that activates the transcription factor NF-kappaB. *Oncogene* 1998;17:1821-6.
  62. Cichon MA, Radisky DC. ROS-induced epithelial-mesenchymal transition in mammary epithelial cells is mediated by NF-kB-dependent activation of Snail. *Oncotarget* 2014;5:2827-38.
  63. Stanisavljevic J, Porta-de-la-Riva M, Batlle R, de Herreros AG, Baulida J. The p65 subunit of NF-kappaB and PARP1 assist Snail1 in activating fibronectin transcription. *J Cell Sci* 2011;124:4161-71.
  64. Bhat KP, Balasubramanian V, Vaillant B, Ezhilarasan R, Hummelink K, Hollingsworth F, et al. Mesenchymal differentiation mediated by NF-kappaB promotes radiation resistance in glioblastoma. *Cancer Cell* 2013;24:331-46.
  65. Dancea HC, Shareef MM, Ahmed MM. Role of Radiation-induced TGF-beta Signaling in Cancer Therapy. *Mol Cell Pharmacol* 2009;1:44-56.

Abstract (IN KOREAN)

교모세포종에서 cystine/glutamate transporter (system  $x_c^-$ )의  
억제에 의한 방사선 감수성 향상 및 종양 증식 억제 효과

<지도교수 김 철 훈>

연세대학교 대학원 의과학과

윤 홍 인

교모세포종은 근치적 절제술 후 방사선 치료 및 테모졸로마이드 (Temozolomide)의 병용 치료에도 불구하고 가장 예후가 불량한 뇌 종양으로 이를 극복하기 위한 새로운 치료 방침이 필요하다. System  $x_c^-$ 는 1 대 1 비율로 글루타메이트 (glutamate)를 세포 밖으로 내보냄과 동시에 시스틴 (cystine)을 세포 안으로 흡수하는 수송체로, xCT (SLC7A11)라는 경쇄 (light-chain subunit)와 CD98hc (SLC3A2)라는 중쇄 (heavy chain subunit)로 구성되어 있다. System  $x_c^-$ 에 의해 흡수된 세포 내 시스틴은 세포 안에서 가장 중요한 항산화제 (antioxidant)인 글루타티온 (glutathione, GSH)을 합성한다. 이는 교모세포종을 포함한 암세포의 생존과 증식에 기여함이 익히 알려져 있다. 이에 system  $x_c^-$ 의 억제가 방사선 치료와 병용하였을 때, 방사선으로 인한 활성산소 (reactive oxygen

species)에 의한 방사선 치료 효과가 증대되고, 종양 증식을 억제시키는 효과도 가져올 수 있다고 가설을 설정하였다.

이 연구는 system  $x_c^-$ 의 억제가 교모세포종의 방사선 감수성을 증가시키고, 교모세포종의 증식과 주변 침범을 억제할 수 있음을 보여주었다. System  $x_c^-$ 의 억제는 교모세포종 세포주들에서 세포 내 클루타티온의 감소를 유도하며, 방사선과 병용시 방사선 단독 처치 군보다 교모세포종 세포들의 디옥시리보핵산 (DNA) 두 가닥 파손(DSB; double strand break)의 양을 증가시켰다. 또한 각 방사선 조사량에서 system  $x_c^-$ 를 억제한 군의 생존 분획 (surviving fraction)이 유의하게 낮았다.

한편, 방사선은 교모세포종에서 간엽성 (mesenchymal) 이행 (transition) 표지자들을 증가시켜서 세포 이동을 증가시킬 수 있는데, 이 연구에서 그 증거로 우리는 방사선 조사 후 교모세포종 세포주에서 간엽성 교모세포종의 The Cancer Genome Atlas (TCGA) 표지자 (marker)인 CD44 와 YKL-40 의 발현량이 증가함을 제시하였다. 방사선으로 인한 간엽성 이행 표지자인 CD44 와 YKL-40 의 발현량 증가가 관찰된 교모세포종 세포주에서 system  $x_c^-$ 의 억제가 교모세포종의 세포 이동을 억제하였다. 그리고 system  $X_c^-$  억제는 교모세포종에서 간엽성 표지자인 SNAIL, vimentin, N-cadherin, alpha-SMA 와 FAP 를 유의하게 감소시켰다. 추가로, 교모세포종 환자의 수술 조직을 이용한 면역 조직 화학 염색 실험에서, system  $x_c^-$ 의 발현량이 예후가 좋지 않은 간엽성 교모세포종에서 높았음을 관찰하였다.

결론적으로 이 연구는 system  $x_c^-$ 의 억제가 방사선과 병용하였을 때 시스템의 흡수와 글루타티온 합성의 감소를 유발하고, 이로 인하여 방사선으로 인한 디옥시리보핵산 손상이 증가함을 관찰하였다. 이는 system  $x_c^-$ 의 억제가 교모세포종의 방사선 감수성을 향상시킬 수 있음을 시사한다. 게다가 system  $x_c^-$ 의 억제가 방사선 유도 세포 이동을 방해하며, 간접성 이행 표지자들도 영향을 주었음을 관찰하였다. 이 모든 결과를 미루어 볼 때, 이 연구는 방사선과 system  $x_c^-$ 의 병용치료가 예후가 좋지 않은 교모세포종에서의 치료 성적 향상에 기여할 수 있음을 시사한다.



---

핵심되는 말: System  $x_c^-$ , 시스템/글루타메이트 수송체, 방사선, 방사선감수성, 세포 이동

## PUBLICATION LIST

1. Lee KJ, **Yoon HI**, Chung MJ, Park JY, Bang S, Park SW, et al. A Comparison of Gastrointestinal Toxicities between Intensity-Modulated Radiotherapy and Three-Dimensional Conformal Radiotherapy for Pancreatic Cancer. *Gut Liver* 2015.
2. **Yoon HI**, Park KH, Lee EJ, Keum KC, Lee CG, Kim CH, et al. Overexpression of SOX-2 is Associated with Better Overall Survival in Squamous Cell Lung Cancer Patients Treated with Adjuvant Radiotherapy. *Cancer Res Treat* 2015.
3. Chung Y, **Yoon HI**, Ha JS, Kim S, Lee IJ. A Feasibility Study of a Tilted Head Position in Helical Tomotherapy for Fractionated Stereotactic Radiotherapy of Intracranial Malignancies. *Technol Cancer Res Treat* 2015;14:475-82.
4. **Yoon HI**, Chung Y, Chang JS, Lee JY, Park SJ, Koom WS. Evaluating Variations of Bladder Volume Using an Ultrasound Scanner in Rectal Cancer Patients during Chemoradiation: Is Protocol-Based Full Bladder Maintenance Using a Bladder Scanner Useful to Maintain the Bladder Volume? *PLoS One* 2015;10:e0128791.
5. Im JH, **Yoon HI**, Kim S, Nam EJ, Kim SW, Yim GW, et al. Tailored radiotherapeutic strategies for disseminated uterine cervical cancer patients. *Radiat Oncol* 2015;10:77.
6. **Yoon HI**, Song KJ, Lee IJ, Kim DY, Han KH, Seong J. Clinical Benefit of Hepatic Arterial Infusion Concurrent Chemoradiotherapy in Locally Advanced Hepatocellular Carcinoma: A Propensity Score Matching Analysis. *Cancer Res Treat* 2015.
7. **Yoon HI**, Cha J, Keum KC, Lee HY, Nam EJ, Kim SW, et al. Treatment

outcomes of extended-field radiation therapy and the effect of concurrent chemotherapy on uterine cervical cancer with para-aortic lymph node metastasis. *Radiat Oncol* 2015;10:18.

8. **Yoon HI**, Seong J. Multimodality treatment involving radiotherapy for advanced liver-confined hepatocellular carcinoma. *Oncology* 2014;87 Suppl 1:90-8.
9. Chang JS, Koom WS, Lee Y, **Yoon HI**, Lee HS. Postoperative adjuvant chemoradiotherapy in D2-dissected gastric cancer: is radiotherapy necessary after D2-dissection? *World J Gastroenterol* 2014;20:12900-7.
10. **Yoon HI**, Lee IJ, Han KH, Seong J. Improved oncologic outcomes with image-guided intensity-modulated radiation therapy using helical tomotherapy in locally advanced hepatocellular carcinoma. *J Cancer Res Clin Oncol* 2014;140:1595-605.
11. **Yoon HI**, Koom WS, Kim YB, Min BS, Lee KY, Kim NK, et al. Predicting the pathologic response of locally advanced rectal cancer to neoadjuvant concurrent chemoradiation using enzyme-linked immunosorbent assays (ELISAs) for biomarkers. *J Cancer Res Clin Oncol* 2014;140:399-409.
12. Jeong YT, Shim J, Oh SR, **Yoon HI**, Kim CH, Moon SJ, et al. An odorant-binding protein required for suppression of sweet taste by bitter chemicals. *Neuron* 2013;79:725-37.
13. **Yoon HI**, Chang JS, Lim JS, Noh SH, Hyung WJ, An JY, et al. Defining the target volume for post-operative radiotherapy after D2 dissection in gastric cancer by CT-based vessel-guided delineation. *Radiother Oncol* 2013;108:72-7.
14. Cha H, **Yoon HI**, Lee IJ, Koom WS, Han KH, Seong J. Clinical factors related to recurrence after hepatic arterial concurrent chemoradiotherapy

- for advanced but liver-confined hepatocellular carcinoma. *J Radiat Res* 2013;54:1069-77.
15. Chung Y, **Yoon HI**, Keum KC, Kim JH, Choi WH, Nam KC, et al. Effect of belly board with bladder compression device on small bowel displacement from the radiotherapy field for rectal cancer. *Onkologie* 2013;36:241-6.
  16. Chang JS, **Yoon HI**, Cha HJ, Chung Y, Cho Y, Keum KC, et al. Bladder filling variations during concurrent chemotherapy and pelvic radiotherapy in rectal cancer patients: early experience of bladder volume assessment using ultrasound scanner. *Radiat Oncol J* 2013;31:41-7.
  17. Yim YS, Kwon Y, Nam J, **Yoon HI**, Lee K, Kim DG, et al. Slitrxs control excitatory and inhibitory synapse formation with LAR receptor protein tyrosine phosphatases. *Proc Natl Acad Sci U S A* 2013;110:4057-62.
  18. Chung Y, **Yoon HI**, Kim JH, Nam KC, Koom WS. Is helical tomotherapy accurate and safe enough for spine stereotactic body radiotherapy? *J Cancer Res Clin Oncol* 2013;139:243-8.
  19. Chung Y, **Yoon HI**, Kim YB, Ahn SK, Keum KC, Suh CO. Radiation pneumonitis in breast cancer patients who received radiotherapy using the partially wide tangent technique after breast conserving surgery. *J Breast Cancer* 2012;15:337-43.
  20. **Yoon HI**, Koom WS, Lee IJ, Jeong K, Chung Y, Kim JK, et al. The significance of ICG-R15 in predicting hepatic toxicity in patients receiving radiotherapy for hepatocellular carcinoma. *Liver Int* 2012;32:1165-71.
  21. Chang JS, Wang ML, Koom WS, **Yoon HI**, Chung Y, Song SY, et al.

High-dose helical tomotherapy with concurrent full-dose chemotherapy for locally advanced pancreatic cancer. *Int J Radiat Oncol Biol Phys* 2012;83:1448-54.

22. Kim JW, Seong J, Yun M, Lee IJ, **Yoon HI**, Cho HJ, et al. Usefulness of positron emission tomography with fluorine-18-fluorodeoxyglucose in predicting treatment response in unresectable hepatocellular carcinoma patients treated with external beam radiotherapy. *Int J Radiat Oncol Biol Phys* 2012;82:1172-8.
23. Shin SJ, **Yoon HI**, Kim NK, Lee KY, Min BS, Ahn JB, et al. Upfront systemic chemotherapy and preoperative short-course radiotherapy with delayed surgery for locally advanced rectal cancer with distant metastases. *Radiat Oncol* 2011;6:99.

